AN ABSTRACT OF THE THESIS OF

Jenna L. Wilson for the degree of Honors Baccalaureate of Science in Bioengineering presented on June 1, 2010. Title: Enhanced Delivery of Cryoprotectant Chemicals to Cultured Neurons.

Abstract approved:

Adam Higgins

Due to the many advances in the areas of biotechnology and medicine, the need for long-term storage and stabilization of biological materials is rapidly increasing. The field of biopreservation is attempting to address these issues by finding ways to maintain the integrity and functionality of proteins, cells, and organs while storing them outside of their native environment. Neurons have been chosen for investigation based on their potential as electrically active sensors and promise for use in cell-based devices. This thesis will focus on the delivery of cryoprotectant chemicals (CPAs), used to prevent damage to the cells during freezing, to cultured neurons prior to cryopreservation. The addition and removal of CPAs can cause serious cell damage due to their creation of an anisotonic environment for cells. Therefore, the development of successful cryopreservation procedures is critically dependent on the method used for addition and removal of CPAs. In order to determine the optimal way to deliver CPAs to neurons, the membrane permeability parameters and osmotic tolerance limits of the cells were determined. The permeability coefficients for water and the cryoprotectants DMSO, propylene glycol, and ethylene glycol were determined using a fluorescence quenching method. Results of the osmotic tolerance experiments showed that at least 50% cell viability was maintained between 25 and 3000 mOsm. Initial feasibility studies of a method of adding CPAs to cells by gradually increasing the concentration (rather than a typical stepwise procedure) were also performed.

Key Words: Cryopreservation, Cryoprotectants, Neurons
Corresponding e-mail address: jennawilson88@gmail.com

©Copyright by Jenna L. Wilson
June 1, 2010
All Rights Reserved

Enhanced Delivery of Cryoprotectant Chemicals to Cultured Neurons

by

Jenna L. Wilson

A PROJECT

submitted to

Oregon State University

University Honors College

in partial fulfillment of
the requirements for the
degree of

Honors Baccalaureate of Science in Bioengineering (Honors Scholar)

Presented June 1, 2010
Commencement June 12, 2010

Honors Baccalaureate of Science in Bioengineering project of Jenna L. Wilson presented on June 1, 2010.

APPROVED:

Mentor, representing Bioengineering

Committee Member, representing Bioengineering

Committee Member, representing Bioengineering

Head, School of Chemical, Biological, and Environmental Engineering

Dean, University Honors College

I understand that my project will become part of the permanent collection of Oregon State University, University Honors College. My signature below authorizes release of my project to any reader upon request.

Jenna L. Wilson, Author

ACKNOWLEDGEMENTS

I would like to thank the following people for their help and support toward this thesis:

> My mentor, Dr. Adam Higgins, for providing me with the opportunity to work on this project and for all of his guidance along the way.
>
> Allyson Fry for being a member of my committee and more importantly for her endless help in the lab. A majority of the cell culture and fluorescence quenching experiments were performed by Allyson, and she has been a great help with every aspect of this project.
>
> Dr. Christine Kelly for being on my committee and providing valuable feedback about my project.
>
> Dr. Phil Harding for his additional insight and advice about the project.
>
> Rachel Bywater and Rob Zarfas for their contributions toward the thesis as a part of our senior design project.

In addition, I would like to thank the OSU office of Undergraduate Research, Innovation, Scholarship & Creativity (URISC) for partially funding my research.

TABLE OF CONTENTS

Acknowledgements **Page v**

List of Figures **Page vii**

List of Tables **Page ix**

List of Appendix Tables **Page x**

Chapter 1: Introduction and background **Page 1**
- Cell membrane permeability and transport Page 2
- Cryopreservation process Page 7
  - Addition of cryoprotectant chemicals Page 7
  - Freezing Page 10
  - Storage Page 12
  - Thawing Page 13
  - Removal of cryoprotectant chemicals Page 13

Chapter 2: Determination of membrane permeability parameters **Page 15**
- Experimental methods Page 16
  - Cell culture Page 16
  - Solution preparation Page 16
  - Fluorescence quenching technique Page 16
- Experimental results and discussion Page 18

Chapter 3: Determination of osmotic tolerance limits **Page 23**
- Experimental methods Page 23
  - Cell culture Page 23
  - Solution preparation Page 23
  - Phase contrast imaging Page 24
  - Cell exposure to solution Page 24
  - Live/dead staining assay Page 25
- Experimental results and discussion Page 27

Chapter 4: Development of a novel CPA addition and removal method **Page 32**
- Intensity vs. dye concentration calibration curve Page 33
- Experimental results and discussion Page 34

Chapter 5: Conclusions and future directions **Page 38**

References **Page 39**

Appendices **Page 41**
- Appendix I: Osmotic tolerance raw data Page 42
- Appendix II: Statistical analyses Page 45

LIST OF FIGURES

Figure 1.1. *Cells exposed to hypertonic solutions ($C_{out} > C_{in}$) will shrink as water leaves the cell, cells exposed to isotonic solutions ($C_{out} = C_{in}$) will remain the same volume, and cells exposed to hypotonic ($C_{out} < C_{in}$) solutions will swell as water enters the cell. The osmotically inactive volume (V_b) remains the same.* **Page 5**

Figure 1.2. *The damage caused to cells is dependent on the freezing rate. When the cells are cooled slowly, solution effects cause most of the damage. When the cells are cooled rapidly, the formation of intracellular ice causes most of the damage.* **Page 11**

Figure 1.3. *The optimal freezing rate can vary dramatically with cell type. In this study, marrow stem cells, yeast, Chinese hamster cells, and human red blood cells (all in suspension) were cooled to -196°C, then rapidly thawed. The optimal cooling rate varies from 1.6°C/min for marrow stem cells to 3000°C/min for human red blood cells. (From Mazur, 1970).* **Page 12**

Figure 2.1. *A schematic of the flow chamber used in experiments for determining cell membrane permeability. The base acts as a heat exchanger to allow temperature control.* **Page 17**

Figure 2.2. *Cells are seeded onto a glass cover slip which is placed face down on the flow chamber to create a micro-channel. Solutions can then be passed through the channel while the microscope and camera measure the change in fluorescent intensity with time.* **Page 18**

Figure 2.3. *Data is adjusted to account for decreasing fluorescence intensity with time. The intensity is also normalized to isotonic conditions at the beginning and end of the experiment.* **Page 19**

Figure 2.4. *The relationship between relative fluorescent intensity and relative volume change with constants derived using MatLab.* **Page 20**

Figure 2.5. *An example of the plot used to determine the permeability activation energy. This graph gives the water permeability activation energy in the presence of ethylene glycol. The slope of the graph is multiplied by the ideal gas constant in order to determine the activation energy.* **Page 22**

Figure 3.1. *A typical phase contrast image of the NS1 cells before any solution has been applied.* **Page 24**

Figure 3.2. *The mechanism of action for the "live" stain. Calcein-AM is converted to calcein inside the cell, a fluorescent molecule which emits green light when excited by green light.* **Page 25**

Figure 3.3. *The mechanism of action for the "dead" stain. Ethidium homodimer is only able to permeate the membranes of dead cells, where it intercalates with the DNA. It emits red dye when excited with blue light.* **Page 26**

Figure 3.4. *A typical live stain image (left) and dead stain image (right) of the NS1 cells.* **Page 26**

Figure 3.5. *The percentage of live cells when calculated by dividing the number of live cells by the total number of live and dead cells. The error bars represent the standard error of the mean of the quadruplicate measurement.* **Page 27**

LIST OF FIGURES (continued)

Figure 3.6. *Phase contrast images were taken of the overnight samples on Day 1 (before any solution was applied) and on Day 2 (after solution was applied but before live/dead staining). This figure shows the percent difference in cell density from Day 1 to Day 2. Those cells that were exposed to solutions at or near isotonic conditions showed growth, while those cells that were exposed to solutions far from isotonic conditions showed a loss of cells, indicating that cells were becoming detached.* **Page 28**

Figure 3.7. *In order to account for detached cells, the data was for each solution was normalized to the control (300 mOsm isotonic solution). The error bars represent the standard error of the mean of the quadruplicate measurement.* **Page 29**

Figure 3.8. *The relative change in the osmotically active cell volume with exposure to different extracellular osmolarities, as predicted by the Boyle-van't Hoff relationship.* **Page 31**

Figure 4.1. *A novel method for adding and removing CPAs to and from cells would utilize a constantly changing CPA concentration rather than a stepwise change.* **Page 32**

Figure 4.2. *A calibration curve was created to determine the linear region of intensity vs. dye concentration. Low concentrations did not give significantly different intensity values, as seen in the left figure. The linear region is shown on the right figure and appears to be in the range of 2-16% dye.* **Page 34**

Figure 4.3. *Visual representations of two commonly encountered problems. In the figure on the left (a), a lag time is experienced at the beginning of pumping. In the figure on the right (b), the syringe gets stuck and jerky due to a wearing down of the lubrication.* **Page 35**

Figure 4.4. *The intensity data (converted to concentration through the linear relationship) versus time using the syringe pumps to vary the concentration of dye in a controlled manner.* **Page 36**

Figure 4.5. *The salt concentration data versus time using the syringe pumps to vary the concentration of salt solution in a controlled manner.* **Page 37**

LIST OF TABLES

Table 2.1. *Permeability parameters for DMSO, propylene glycol (PG), and ethylene glycol (EG) at three different temperatures.* **Page 21**

Table 2.2. *Hydraulic conductivity, which describes the membrane permeability to water, when in conjunction with DMSO, propylene glycol (PG), and ethylene glycol (EG) at three different temperatures.* **Page 21**

Table 2.3. *The Arrhenius activation energies for water and CPA permeability* **Page 22**

LIST OF APPENDIX TABLES

Table AI.1. *Raw data from osmotic tolerance tests for overnight samples (1 of 4)* **Page 42**

Table AI.2. *Raw data from osmotic tolerance tests for overnight samples (2 of 4)* **Page 42**

Table AI.3. *Raw data from osmotic tolerance tests for overnight samples (3 of 4)* **Page 43**

Table AI.4. *Raw data from osmotic tolerance tests for overnight samples (4 of 4)* **Page 43**

Table AI.5. *Raw data from osmotic tolerance tests for instant samples (1 of 2)* **Page 44**

Table AI.6. *Raw data from osmotic tolerance tests for instant samples (2 of 2)* **Page 44**

Table AII.1. *T-test comparison of instant and overnight osmotic tolerance data* **Page 45**

Table AII.2. *ANOVA comparison of instant osmotic tolerance solutions* **Page 45**

Table AII.3. *Multiple range testing (LSD) of instant osmotic tolerance solutions. An asterisk has been placed next to 10 pairs, indicating that these pairs show statistically significant differences at the 95.0% confidence level.* **Page 45**

Table AII.4. *ANOVA comparison of overnight osmotic tolerance solutions* **Page 46**

Table AII.5. *Multiple range testing (LSD) of overnight osmotic tolerance solutions. An asterisk has been placed next to 13 pairs, indicating that these pairs show statistically significant differences at the 95.0% confidence level.* **Page 46**

ENHANCED DELIVERY OF CRYOPROTECTANT CHEMCIALS TO CULTURED NEURONS

CHAPTER 1 – INTRODUCTION AND BACKGROUND

Due to the many advances in the areas of biotechnology and medicine, the need for long-term storage and stabilization of biological materials is rapidly increasing. For example, cell-based biosensors have the capability to perform medical diagnosis, detect environmental toxins, and complete drug screening, among other things. However, the success of these devices is dependent on the long-term stabilization and viability of the sensing cells. The field of biopreservation is attempting to address these issues by finding ways to maintain the integrity and functionality of proteins, cells, and organs while storing them outside of their native environment. Neurons have been chosen for investigation based on their potential as electrically active sensors and promise for use in cell-based devices. There has been significant research regarding the development of these devices but very little research directed toward the problem of mass producing these products while maintaining the viability of the incorporated living cells. Cells in suspension have been successfully stored using cryopreservation for many years. However, a limited amount of progress has been made in the cryopreservation of adherent cells and tissues. This project will attempt to help remedy these omissions.

This thesis will focus on the role of cryoprotectant chemicals (CPAs) in the cryopreservation of cultured neurons. These chemicals are used to prevent damage to the cells during freezing. However, the addition and removal of CPAs can cause serious cell damage due to their creation of an anisotonic environment for cells. Therefore, the development of successful cryopreservation procedures is critically dependent on the method used for addition and removal of CPAs. In order to determine an optimal way to deliver CPAs to neurons, the membrane permeability parameters and osmotic tolerance limits of the cells must be determined.

This paper is structured in such a way to provide a thorough physical understanding of the examined system. This introduction (Chapter 1) provides an overview of the relevant areas of cell membrane permeability and transport. It also describes the cryopreservation process and the possible mechanisms of damage associated with each step. Chapter 2 provides information and results regarding the determination of membrane permeability parameters using the fluorescence quenching technique. In Chapter 3, the experiments for establishment of osmotic tolerance limits for the cells are detailed and the results discussed. Chapter 4 describes a novel method of adding CPAs to cells in which the concentration is changed linearly rather than in a stepwise manner. The conclusions and possible future work based on the ideas presented are summarized in Chapter 5.

Cell membrane permeability and transport:

In order to grasp the mechanisms of damage during CPA addition and cryopreservation, basic principles of membrane permeability and transport must be understood. The kinetics of water transport across the cell membrane is the main determinant of whether a cell survives the cryopreservation process. The cell membrane is a semi-permeable barrier that defines the boundary between the cytoplasm of the cell and the extracellular environment. It consists of a phospholipid bilayer that acts as a relatively impermeable barrier to many molecules, particularly those that are polar, hydrophilic, or charged. Water is able to diffuse through the membrane, along with small non-polar molecules (Alberts et al., 2008).

The permeability of a molecule through the lipid bilayer is proportional to the concentration difference on the two sides of the membrane and the permeability coefficient of the molecule. The permeability coefficient (P) is defined as the number of molecules of the diffusing species crossing the membrane per unit time and unit area of the membrane when a unit concentration difference is applied across the membrane. It has units of length per time, so it can be thought of as a rate (Stein, 1967). The permeability coefficient can be related to the diffusion coefficient through the membrane (D), the partition coefficient (K), and thickness of the membrane (δ), shown in *Equation 1.1*. The partition coefficient describes the molecule's solubility in lipids.

$$P_i = \frac{K_i D_i}{\delta} \qquad [1.1]$$

The higher the permeability coefficient is, the more readily the molecule can diffuse through the membrane. For example, the permeability coefficient of water through the lipid bilayer is approximately 5 x 10^{-3} cm/s, while the permeability coefficient for Na^+ is approximately 1 x 10^{-12} cm/s (Verkman, 2000; Alberts et al., 2008).

The permeability of water has historically been described as a hydraulic conductivity (L_P) rather than as a permeability coefficient. The hydraulic conductivity is a proportionality constant that relates the volumetric water flux to the difference in osmotic pressure on the inside and outside of the cell (Stein, 1967). It can also be thought of as the mechanical filtration capacity of the membrane (McGrath, 1997). The hydraulic conductivity can be related to the permeability coefficient for water (P_w) using the relationship in *Equation 1.2*. In this equation, v_w refers the molar water volume, R refers to the universal gas constant, and T refers to the absolute temperature. The hydraulic conductivity of a cell membrane will be reduced if the cell has fewer aquaporin water channels (Solenov et al., 2004).

$$L_p = \frac{v_w D_w K_w}{\delta R T} \qquad [1.2]$$

Membrane permeability also has a strong dependence on temperature. The relationship is based on the Arrhenius activation energy (E_a) which provides a measure of the energy barrier to water transport across the membrane (Verkman, 2000). The relationship is defined in *Equation 1.3*, where L_{pg} is the hydraulic conductivity at a reference temperature (T_{ref}) (Levin et al., 1976).

$$L_p(t) = L_{pg} \exp\left[-\frac{E_A}{R}\left(\frac{1}{T} - \frac{1}{T_{ref}}\right)\right] \qquad [1.3]$$

Water and solute transport are directly related to the volume of the cell, therefore changes in cell volume can be used to study permeability parameters. Many mathematical models have been derived that describe the movement of water and solutes across the cell membrane. Often, these models incorporate the osmotic pressure of the system. Osmotic pressure is a phenomenon that occurs due to the tendency of water to want to move across a semi-permeable barrier into a solution containing a higher concentration of an impermeable solute. The "pressure" refers to the pressure that must be applied in order to stop the movement of the water across the membrane. As a result, water will want to move from an area of low osmotic pressure to an area of high osmotic pressure. The osmotic pressure (Π) can be related to the concentration of impermeable solute (C_s) with the Morse relationship, shown in *Equation 1.4*, where i is the van't Hoff factor. The van't Hoff factor is roughly equal to the number of discrete ions in the molecule, usually one.

$$\Pi = iC_s RT \qquad [1.4]$$

In a normal physiological state, a homeostatic mechanism known as osmoregulation maintains an equal osmotic pressure inside and outside the cell. In this condition, the cell is said to be at an isotonic state, and the cell volume remains relatively constant. In physiological systems, the concentration of an isotonic solution is approximately 300 mOsm.

When a cell is exposed to an anisotonic solution, water is forced to enter or leave the cell due to osmotic pressure differences. If the extracellular solution has a higher concentration of solute than the intracellular solution, it is referred to as a hypertonic solution. Water will leave the cell faster than it enters it, causing the cell to shrink. If the extracellular solution has a lower concentration of solute than the intracellular solution, it is referred to as a hypotonic solution. Water will enter the cell faster than it leaves it, causing the cell to swell. These situations are summarized in *Figure 1.1*. Both excessive shrinking and swelling can lead to cell death (Tortora & Derrickson, 2009).

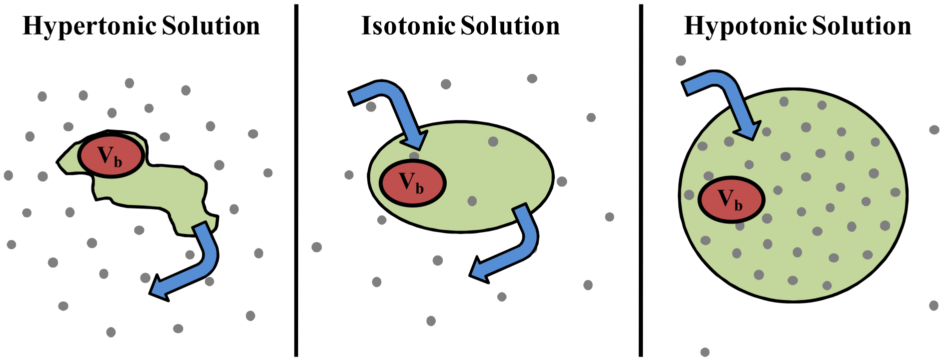

Figure 1.1. *Cells exposed to hypertonic solutions ($C_{out} > C_{in}$) will shrink as water leaves the cell, cells exposed to isotonic solutions ($C_{out} = C_{in}$) will remain the same volume, and cells exposed to hypotonic ($C_{out} < C_{in}$) solutions will swell as water enters the cell. The osmotically inactive volume (V_b) remains the same.*

The total cell volume is made up of an osmotically active volume (V_w) and an osmotically inactive volume (V_b), which contains intracellular solids and macromolecules that will always remain in the cell. The portion of the cell volume that changes as the cell is exposed to anisotonic solutions is the osmotically active cell volume. When the cell is exposed to an anisotonic solution which contains only impermeable solutes, the Boyle-van't Hoff relationship can be applied. This is shown in *Equation 1.5*. V_{wo} refers to the osmotically active volume at isotonic conditions, while Π_o and Π_i refer to the osmotic pressure of isotonic and extracellular conditions, respectively.

$$\frac{V_w}{V_{wo}} = \frac{\Pi_o}{\Pi_e} \qquad [1.5]$$

Combining the concepts of membrane permeability and cell volume change leads to mathematical models of the differential cell volume change with time. The equations can be simplified if the flux of CPA is insignificant in comparison to the flux of water. In this case, the relationship simplifies to *Equation 1.6* (Mazur, 1963; Levin et al., 1976). The A refers to the cellular surface area while the Π_e and Π_i refer to the osmotic pressure of extracellular and intracellular conditions, respectively

$$\frac{dV_w}{dt} = -L_P A(\Pi_e - \Pi_i) \qquad [1.6]$$

If a permeating solute is used, a similar expression can be derived which shows the change in solute volume with time, shown in *Equation 1.7*. The v_S refers to the molar volume of the solute while the M_e and M_i refer to the osmolarities of the extracellular and intracellular solutions, respectively.

$$\frac{dV_S}{dt} = -P_S A v_S \left(M_e - M_i\right) \qquad [1.7]$$

The transient permeability of water and CPA can be described in the coupled differential equations shown in *Equations 1.8* and *1.9*. In these equations, C_o refers to the initial concentration, v_{CPA} refers to the molar volume of CPA in solution, C_e refers to the extracellular concentration, and A refers to the cellular surface area.

$$\frac{d\left(\frac{V_w}{V_{wo}}\right)}{dt} = -\frac{L_P ART}{V_{wo}}\left[\left(C_o + \frac{V_{CPA}}{v_{CPA}V_{wo}}\right)\left(\frac{V_{wo}}{V_w}\right) - C_e\right] \qquad [1.8]$$

$$\frac{d\left(\frac{V_{CPA}}{V_{wo}}\right)}{dt} = \frac{P_{CPA}A}{V_{wo}}\left[v_{CPA}C_{CPA,e} - \left(\frac{V_{CPA}}{V_{wo}}\right)\left(\frac{V_{wo}}{V_w}\right)\right] \qquad [1.9]$$

The water transport model can be further modified to predict the change in cell volume during freezing (Karlsson et al., 1993; Devireddy et al., 2000). This relationship is shown in *Equation 1.10*. The variables in the equation are defined as follows: B is the constant cooling rate (K/min); V_{wo} is the osmotically active volume at isotonic conditions*;* n_s is the number of moles of solute/CPA in solution; φ is the dissociation constant for salts in the cell initially C_i is the initial cell osmolarity; ΔH_f is the latent heat of fusion for water (335 mJ/mg); ρ is the density of water (1000 kg/m^3); T_{ref} is the reference temperature; T is the subzero temperature at which the cell volume is being determined; L_{pg} is the reference membrane permeability at a reference temperature; and E_{Lp} is the apparent activation energy of the cell membrane permeability. It should be noted that this model was developed for single cell systems, not for tissues.

$$\frac{dV}{dt} = -\frac{L_P ART}{B\nu_w}\left[\ln\left(\frac{(V_{wo} - n_s\nu_s)/\nu_w}{(V_{wo} - n_s\nu_s)/\nu_w + \phi_s C_i V_{wo} + n_s}\right) - \frac{\Delta H_f \nu_w \rho}{R}\left(\frac{1}{T_{ref}} - \frac{1}{T}\right)\right] \quad [1.10]$$

The concepts of membrane permeability and transport are vital for understanding the problems associated with the addition of cryoprotectant chemicals and the cryopreservation process. The ability to mathematically model these transport processes enables better optimization of cryopreservation procedures.

Cryopreservation process:

Cryopreservation is a common approach for long-term preservation of viable cells. The general steps in this process are addition of cryoprotectant chemicals (CPAs), freezing, and storage at liquid nitrogen temperature (-196°C), followed by thawing and removal of CPAs when the cells are needed. The basic procedure of each of these steps is described in more detail below. There are two common types of damage during cryopreservation. The first is “solution effects” in which the cell is damaged from dehydration. This type of damage can be attributed to four events which can occur simultaneously: the removal of water as ice, the concentration of solutes, the decrease in cell volume, and the precipitation of solutes. The second major cause of damage is the formation of intracellular ice, in which the cell is lysed due to mechanical damage.

1. Addition of Cryoprotectant Chemicals

Certain organisms, including red blood cells and most microorganisms, can survive freezing at an optimal rate without the addition of cryoprotectant chemicals. However, nucleated mammalian cells required addition of cryoprotectant chemicals (CPAs) prior to freezing in order to minimize damage (Mazur, 1970). CPAs can be divided into two different classes: permeating and non-permeating. Permeating CPAs are able to pass through the cell membrane and include dimethyl sulfoxide (DMSO), ethylene glycol, propylene glycol, and glycerol. Non-permeating CPAs are not able to pass through the cell membrane and include polymers and sugars such as sucrose and trehalose. Though their precise mechanism of action is not known, it is generally believed that permeating CPAs reduce high concentrations of electrolytes in the cell, decreasing the chance of damage due to solution effects (Karlsson, & Toner, 1996). Several other theories regarding a CPA's ability to reduce freezing damage have been proposed.

The first possible mechanism is through colligative cryoprotection, which may occur with permeating CPAs. The idea is that the additional solute within the cell will decrease the vapor pressure of the aqueous solution, therefore reducing the amount of ice formed at a given temperature. Colligative cryoprotection can be enhanced further if the addition of CPA substantially increases the nonaqueous volume of the cell. However, this mechanism alone does not appear to entirely account for the cryoprotection benefits, as high concentrations of CPA would need to be added to achieve the proposed benefits (Meryman, 1974). The addition of high volumes of CPA may cause additional problems due to osmotic pressure and CPA toxicity.

Another possible mechanism is that CPAs provide resistance to volume reduction. An increasing pressure gradient will develop across the cell membrane with increasing external osmolarity. Therefore, the protection due to this mechanism is likely limited to the amount of stress the cell membrane can withstand. A third potential mechanism is the reduction of the critical volume of a cell, defined as the volume at which irreversible damage occurs (Meryman, 1974). While both of these mechanisms could theoretically contribute to cryoprotection, there have been limited experimental observations made to confirm their existence.

For permeating solutes, there is evidence that the presence of CPAs helps to stabilize the structure of biomolecules. Proteins and DNA are vulnerable to damage due to loss of hydrogen bonding with water as the cell is dehydrated. It is believed that certain CPAs may replace the hydrogen bonding that water usually forms with biomolecules, stabilizing proteins and DNAs during the freezing process (Mazur, 1970). Similarly, it is hypothesized that cellular proteins may be stabilized entropically by CPAs if they are preferentially excluded from the protein's hydration shell (Arakawa et al., 1990).

Another proposed mechanism is that permeating CPAs act to raise the glass transition temperature of the intracellular solution. This occurs when high concentrations of cryoprotectants permeate the cell, resulting in an increased viscosity of the extracellular and intracellular solutions (Karlsson & Toner, 1996). In this way, the solution will not actually freeze but will instead be preserved in a sort of flexible, glassy state. This mechanism is the basis for the process of vitrification.

The possible mechanisms previously discussed apply primarily to permeating solutes. The proposed means of protection for non-permeating CPAs, usually polymers or sugars, is slightly different. Since these chemicals are unable to cross the cell membrane, they must act extracellularly. Experimentation shows that non-permeating CPAs reduce cell damage due to solutions effects, so it appears their mechanism of protection is related to impeding or reversing this type of cell injury. Because of this, non-permeating CPAs are best utilized when performing rapid freezing and thawing (Meryman, 1974).

No matter the mechanism of action, cryoprotectants are a necessary component of the cryopreservation process. However, these chemicals themselves can also cause damage to the cells when used in high concentrations. In order to reduce the toxicity, the time and temperature of cell exposure to the CPA, along with the concentration, should be minimized. Major damage can also come from the addition of the CPA to the cell. Because cryoprotectants permeate the cell membrane slower than water does, the cell will lose water through osmosis when exposed to a CPA solution. If a permeating CPA is used, the cell will eventually be restored to its normal volume once the CPA has crossed the membrane and the concentration has equilibrated. However, irreversible damage can occur if the volume changes too drastically before equilibrium is reached. In order to reduce this type of cell damage, CPAs are typically added slowly, with the concentration being increased in a stepwise manner (Karlsson & Toner, 1996). Determining ways to load the cells with the necessary amount of cryoprotectant while maintaining high cell viability is the main focus of this thesis.

2. Freezing

Once the cryoprotectant has been loaded into the cells, freezing can begin. The first step in this process is to seed extracellular ice at a temperature slightly lower than the solution melting point. The intentional initiation of ice formation gives some control over where and what temperature ice first begins to form. If this is not done, ice can form in a spontaneous manner, giving inconsistent cell survival rates (Karlssson & Toner, 1996). As extracellular ice forms, the intracellular solution remains unfrozen in a supercooled state. The supercooled water within the cell has a higher chemical potential than the partially frozen extracellular solution, causing water to leave the cell and freeze externally (Mazur, 1984). Studies have shown that the formation of extracellular ice at high degrees of supercooling can increase the formation of intracellular ice, once of the major reasons cells are destroyed during freezing. This is most likely a result of the increased degree of cooling the cell experiences due to the thermal fluctuations from the release of latent heat during the formation of extracellular ice. It is also due to the delay in cell dehydration, resulting in greater retention of intracellular water that increases the probability of intracellular ice formation (Diller, 1975; Mazur 1977). After the ice is seeded, the cells are typically held at this temperature, allowing them to crystallize as well as thermally and chemically equilibrate (Karlssson & Toner, 1996).

Once the ice has been seeded and the cells have had a chance to equilibrate, the process of cooling the cells to -196°C can begin. Freezing is typically performed at a constant cooling rate with the temperature decreased by a set number of degrees per minute. The rate at which the cells are cooled can dramatically affect the survival rate, as shown in *Figure 1.2*. If the cells are cooled too slowly, water has ample time to leave the cell in order to equilibrate with the extracellular ice. This leads to severe cellular dehydration and damage due to solution effects. However, damage due to intracellular ice formation is reduced. As the cell becomes dehydrated, the increased solute concentration inside the cell depresses the equilibrium melting point so that supercooling of the intracellular solution is reduced. On the other hand, completely different mechanisms of damage can occur if the cells are cooled too rapidly. In this case, supercooling of the cytoplasm quickly increases, causing intracellular ice formation to occur at relatively high temperatures. This formation of intracellular ice dominates cell damage, while solution effects are nearly negligible because the water does not have enough time to leave the cell (Karlsson & Toner, 1996).

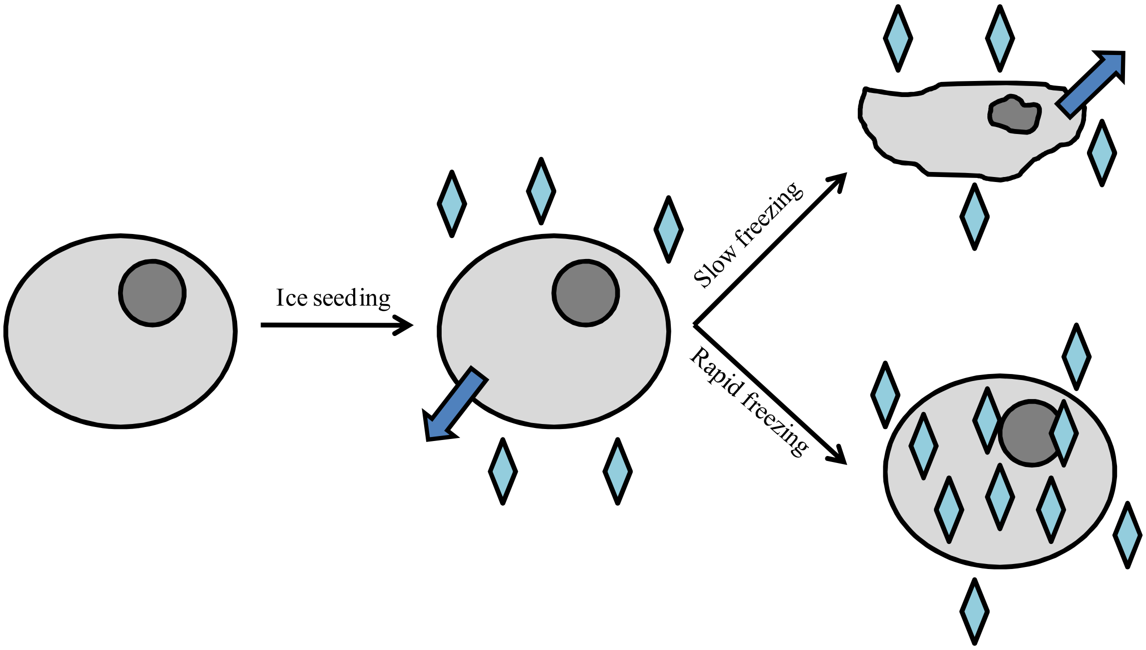

Figure 1.2. *The damage caused to cells is dependent on the freezing rate. When the cells are cooled slowly, solution effects cause most of the damage. When the cells are cooled rapidly, the formation of intracellular ice causes most of the damage.*

In order to determine the optimal cooling rate for cells, the advantages and disadvantages of rapid versus slow cooling rate need to be compromised. The relationship between cooling rate and cellular dehydration can be exploited up to a point in order to control the cell volume and the concentration of the intracellular solution. However, a temperature is reached in which the cell membrane becomes effectively impermeable to water due to the Arrhenius relationship relating the hydraulic conductivity to the temperature (see *Equation 1.3*) (Karlsson et al., 1994).

Different cell types can have dramatically different optimal cooling rates. For a comparison of optimal freezing rate for four different cell types, see *Figure 1.3*. Just between these four cell types (all in suspension), the most favorable cooling rate ranges from 1.6°C/min for marrow stem cells to 3000°C/min for human red blood cells (Mazur, 1970). Due to this wide variation, it is necessary to experimentally confirm the best freezing rate for each cell type to avoid unnecessary cell damage.

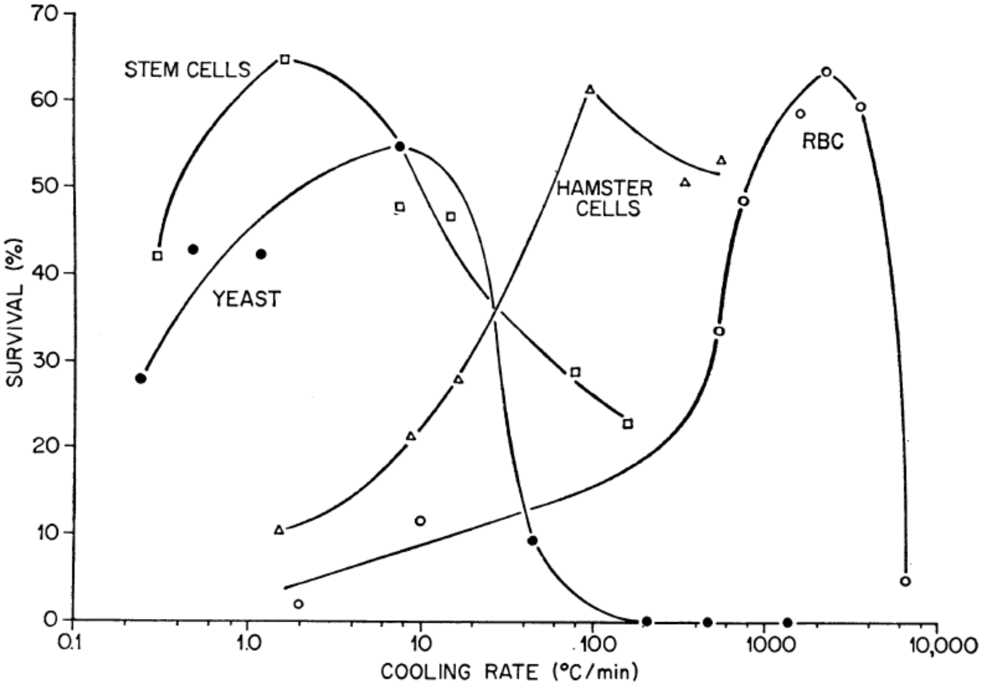

Figure 1.3. *The optimal freezing rate can vary dramatically with cell type. In this study, marrow stem cells, yeast, Chinese hamster cells, and human red blood cells (all in suspension) were cooled to -196°C, then rapidly thawed. The optimal cooling rate varies from 1.6°C/min for marrow stem cells to 3000°C/min for human red blood cells. (From Mazur, 1970).*

3. Storage

Once the cells have been cooled to -196°C (the boiling point of liquid nitrogen), they can be stored in liquid nitrogen for a very long period of time without incurring additional damage. At -196°C and below, no chemical reactions are able to occur due to the lack of thermal energy. The only reactions able to occur are those produced by background radiation or cosmic rays, such as the formation of free radicals or the creation of breaks in macromolecules. However, the cells would have to be stored for 2,000 to 4,000 years before enough damage was achieved to reduce cell viability below 35% (Mazur, 1984).

4. Thawing

Just as cooling the cells at a certain rate can impact their survival, the rate at which they are thawed also impacts cell viability. In general, cells that were cooled rapidly should be warmed rapidly, while cells that were cooled slowly should be warmed slowly. For rapidly cooled cells, additional ice nucleation and crystal formation can arise in the time it takes to reach the equilibrium melting point. In addition, small, harmless intracellular ice crystals that formed during freezing can turn into larger, more destructive ice crystals as the cells are thawed (Karlsson & Toner, 1996). Rapid thawing will reduce the likelihood of cell damage in this manner. For cells that were cooled slowly, there may be a higher concentration of solute in the cell. Therefore, when rapid cooling is used, there will not be enough time for the excess solute to leave the cell, causing the cell to swell and possibly cause cell lysis. Slow thawing will reduce the likelihood of cell damage in this manner (Mazur, 1984).

5. Removal of cryoprotectant chemicals

Before the newly thawed cells can be utilized, any cryoprotectant chemical that was added before freezing must be removed. If cells containing CPA are added directly back to normal physiological media (300 mOsm), osmotic pressure will cause the cells to swell since the water can enter the cell faster than the cryoprotectant can leave it. Therefore, CPA must be slowly diluted out of the cells just as it had to be gradually added (Mazur, 1984).

In every step in the cryopreservation process, transport of water and solutes across the membrane plays a key role in the survival of cells. The method by which cryoprotectant is added and removed is completely dependent on the permeability characteristics of the membrane. The cell membrane is what prevents ice from nucleating in cells at warmer temperatures. The water permeability of the membrane determines how the cells will equilibrate to their environment at low temperature, whether it is through dehydration or formation of intracellular ice. When a cell is damaged, the membrane is often what is compromised (Mazur, 1970). The fundamental relationship between membrane permeability and cell survival during cryopreservation is the premise for this thesis.

CHAPTER 2 – DETERMINATION OF MEMBRANE PERMEABILITY PARAMETERS

Establishing the permeability of the cell membrane to water and cryoprotectant chemicals is essential for development of optimal procedures for adding and removing cryoprotectant chemicals. Each cell type has different permeability parameters due to the variation in membrane composition. The membrane permeability parameters for many cell types in suspension have already been determined. However, due to the limitation of suitable techniques for adherent cells and tissue, membrane characterization has been limited. The permeability of water and solutes through the membranes of cells in suspension cannot be directly correlated to the permeability of adherent cells. It's believed that the disparity in permeability parameters may be due to greater mass transfer limitations and/or from cell-cell tethering (Bischof, 2000).

The primary reason for the lack of permeability data for adherent cells has been the difficulty of measurement. The development of the fluorescence quenching method, utilized in this project to determine the NS1 membrane permeability, came about relatively recently. The technique utilizes the fluorescent dye calcein-acetoxymethyl ester (calcein-AM) to determine cell volume changes. This dye can initially diffuse through the cell membrane, however once inside the cell, esterases cleave off the acetoxymethyl ester groups. Once these side chains are lost, the remaining calcein molecule is impermeable to the membrane and is therefore trapped inside the cell. The intensity of the fluorescence changes as the cell volume changes due to the quenching of calcein fluorescence by a molecule in the cytoplasm. It was initially believed that calcein underwent self-quenching (Haman et al., 2002). However, it is now thought that there are quenching molecules in the cytoplasm of the cell. As the cell shrinks, the calcein molecules become more densely packed, resulting in an increase in quenching and a decrease in fluorescence intensity. As the cell swells, the calcein molecules become more spread out, resulting in a decrease in quenching and an increase in fluorescence intensity (Solenov et al., 2004). Therefore, cell volume changes can be monitored by observing the change in fluorescent intensity. As described in Chapter 1, the change in volume can be directly related to the permeability parameters of the membrane.

In these experiments, the hydraulic conductivity (L_p) and permeability coefficients for three common cryoprotectants – dimethyl sulfoxide (P_{DMSO}), ethylene glycol (P_{EG}), and propylene glycol (P_{PG}) – were determined for the NS1 neural cell line.

Experimental methods:

Cell culture

The cells used in the experiments are from Neuroscreen-1 (NS1) cell line, a subclone of the PC12 cell line which is a standard model system for neurons. NS1 cells were cultured in tissue culture flasks containing DMEM media with horse serum and Pen/Strep at 37°C in a 5% CO_2 environment. NGF-β, a nerve growth factor recombinantly produced in rats (Sigma N2513), was added at a concentration of 50 µg/mL in order to transform the neural progenitor cells into neurons. For the fluorescence quenching experiments, cells were seeded onto 25 mm diameter glass cover slips, coated with poly-L-lysine and collagen. They were cultured in 35 mm Petri dishes for 2 days. Directly before fluorescence quenching, the cells were incubated in PBS containing 1.25 µg/mL calcein-AM for 15 minutes at 37°C.

Solution preparation

In this set of experiments, cells were exposed to three different cryoprotectant chemicals (DMSO, propylene glycol, and ethylene glycol), each at three different concentrations (1 M, 2 M, and 3 M). Each solution began with a 1X PBS solution containing Ca^{2+} and Mg^{2+} with an osmolarity of 300 mOsm (isotonic). The appropriate amount of each cryoprotectant was added, with the final osmolality confirmed using an Advanced Instruments freezing point depression micro-osmometer. The solutions were adjusted to a pH of 7.0.

Fluorescence quenching technique

In order to examine cell volume changes with time, a controlled and observable environment is required. A flow chamber was constructed in order to meet this need, shown in *Figure 2.1*. The base of the chamber acts as a heat exchanger so that the experiments can be temperature-controlled. A water bath flows into the base, and the tubing containing the flow solutions is exposed to the water bath for the required heat transfer time.

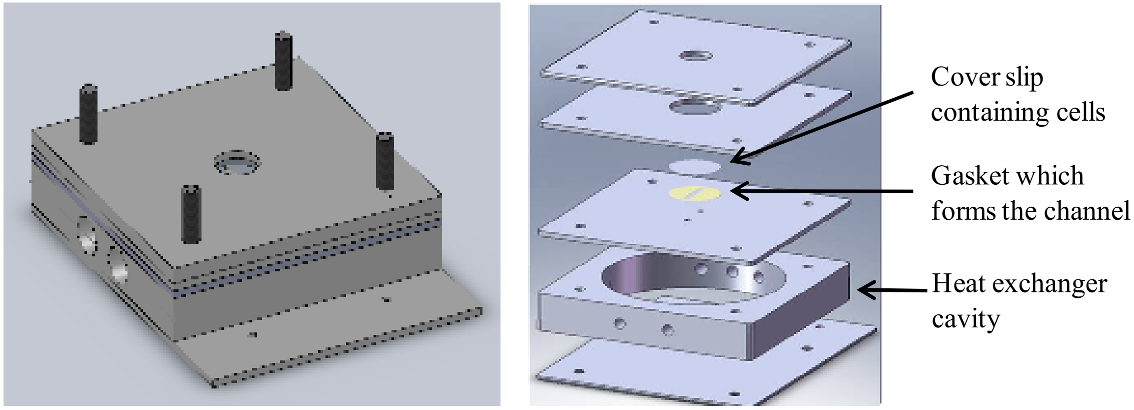

Figure 2.1. *A schematic of the flow chamber used in experiments for determining cell membrane permeability. The base acts as a heat exchanger to allow for temperature-control.*

A cover slip seeded with cells is placed face down over a thin opening, creating a micro-channel. Solutions of varying compositions and concentrations are passed through this channel, as shown in *Figure 2.2*. There are two inputs to the channel, each of which is primed to the channel opening so that the solution the cells are exposed to can be changed very quickly. The flow of the solutions is controlled using a syringe pump along with Syringe Pump Pro software. There is an open region in the flow chamber above the channel to allow for viewing by the microscope objective. The fluorescence intensity is recorded using Qicam camera with 0.5x coupler attached to a compound microscope with a green fluorescent filter. Image Pro software is used to manage the collected data. A 50 millisecond exposure time is used, and images are recorded at a rate of one per second.

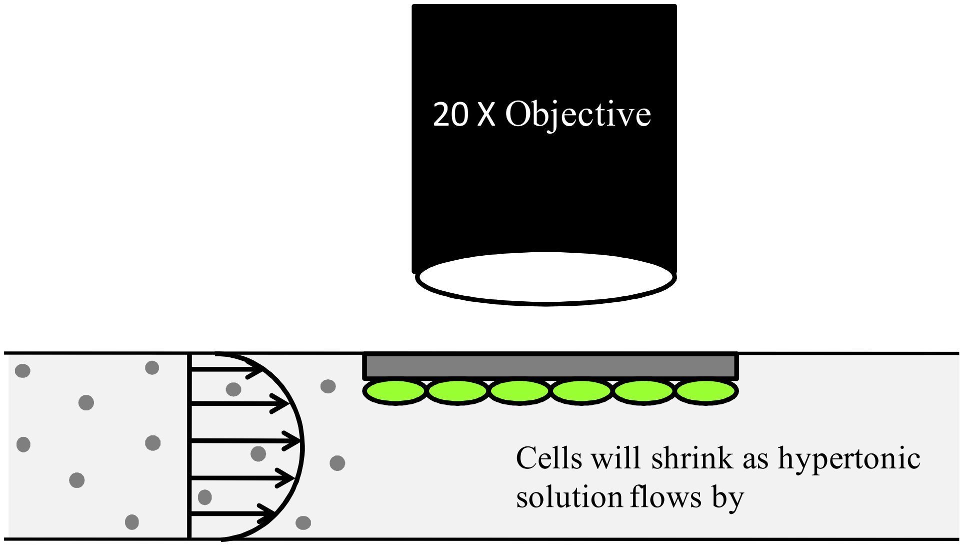

Figure 2.2. *Cells are seeded onto a glass cover slip which is placed face down on the flow chamber to create a micro-channel. Solutions can then be passed through the channel while the microscope and camera measure the change in fluorescent intensity with time.*

In these experiments, the cover slip containing the cell monolayer was placed into the flow chamber while carefully avoiding the introduction of bubbles. Isotonic PBS solution was perfused through the flow chamber at a rate of 20 mL/hr for 5-10 minutes to ensure equilibrium within the chamber. After this time has passed, the flow rate was increased to 200 mL/min and image collection was started. Once the isotonic solution has perfused for a set amount of time, the syringe pumps switch so that the cells are exposed to an anisotonic solution. This solution flows for a set amount of time before perfusion is changed back to isotonic solution.

Experimental results and discussion:

In this set of experiments, cells were exposed to three different cryoprotectant chemicals (DMSO, propylene glycol, and ethylene glycol), each at three different concentrations (1 M, 2 M, and 3 M) and three different temperatures (4°C, 21°C, and 37°C).

The fluorescence intensity data must first be adjusted to account for fluorescent fading caused by photo-bleaching and leaking of intracellular calcein dye. This is accomplished by assuming that the initial and final isotonic conditions should correspond to the same fluorescent intensity. The entire data set is then altered to reflect this, as shown in *Figure 2.3*. The fluorescence intensity is also normalized so that it is equal to one at isotonic conditions.

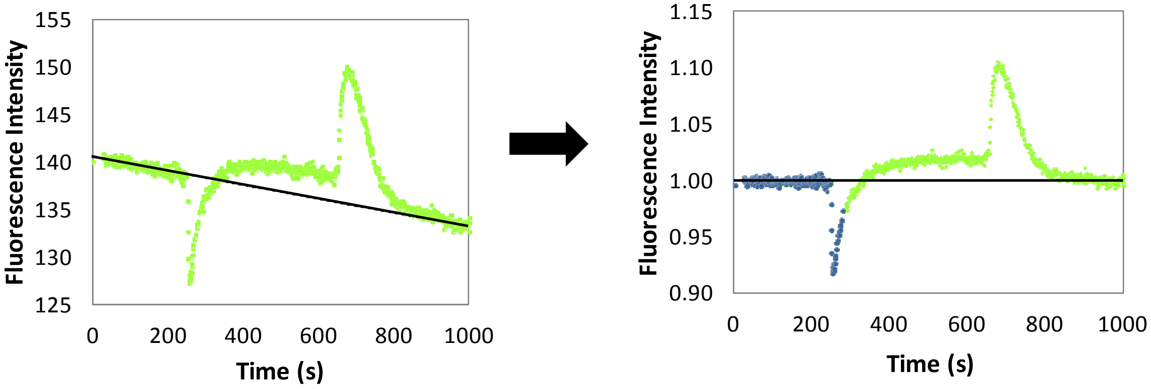

Figure 2.3. *Data is adjusted to account for decreasing fluorescence intensity with time. The intensity is also normalized to isotonic conditions at the beginning and end of the experiment.*

The next necessary step is converting the intensity data into volume data. This is done through utilization of the Stern-Volmer relationship, shown in *Equation 2.1*. In this equation, F_o refers to the fluorescent intensity with no quencher, F refers to the fluorescent intensity in the presence of quencher, K is the quenching constant, and Q is the quencher concentration.

$$\frac{F_o}{F} = 1 + KQ \qquad [2.1]$$

In order to apply this, the fluorescence intensity due to both the osmotically active volume and the osmotically inactive volume must be considered. When the Boyle-v'ant Hoff relationship is applied (see *Equation 1.5*), a relationship between fluorescent intensity and the change in the osmotically active volume can be derived. This relationship is shown in *Equation 2.2*, where F_I is the fluorescent intensity at isotonic conditions, V_w is the osmotically active volume, V_{wo} is the osmotically inactive volume at isotonic conditions, K_A is the quenching constant for the osmotically active volume, Q_I is the quencher concentration under isotonic conditions, F_{oA} is the fluorescent intensity contributed by the osmotically active volume with no quencher present, and F_B is the fluorescent intensity contributed by the osmotically inactive volume.

$$\frac{F}{F_I} = \frac{\left(\frac{V_w}{V_{wo}}\beta + \alpha\right)(1+\alpha)}{\left(\frac{V_w}{V_{wo}} + \alpha\right)(\beta+\alpha)} \qquad [2.2]$$

where $\alpha = K_A Q_I$ and $\beta = \frac{F_{oA}}{F_B} + 1$

A MatLab program is used to fit the constants α and β given the fluorescence intensity data. The results of the volume calibration are shown in *Figure 2.4*.

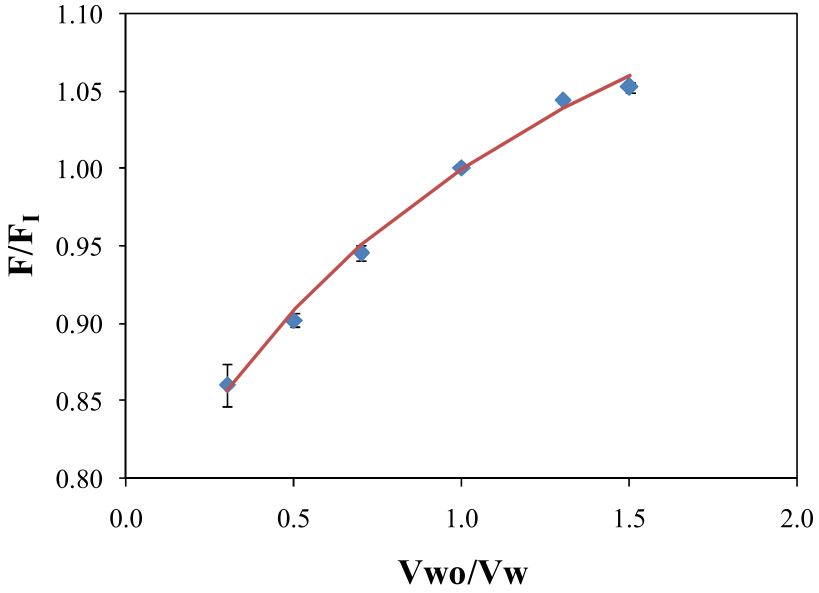

Figure 2.4. *The relationship between relative fluorescent intensity and relative volume change with constants derived using MatLab.*

Once the relationship between fluorescent intensity and volume change has been established, MatLab programs are then used to determine the permeability parameters of the cells. An exponential decay model is fit to the data preceding the change from isotonic to hypotonic conditions to the data in which isotonic volume is once more achieved. This area is highlighted in

Figure 2.3. Using this data and *Equations 1.8* and *1.9*, the program uses an ODE solver while determining parameters which minimize the error. The end products of the program are the lumped permeability parameters $P_{CPA}A/V_{wo}$ and L_pA/V_{wo}. These results are shown in *Tables 2.1* and *2.2*.

Table 2.1. *Permeability parameters for DMSO, propylene glycol (PG), and ethylene glycol (EG) at three different temperatures.*

Permeability (µm/s)	**4°C**	**21°C**	**37°C**
$P_{DMSO}A/V_{wo}$	0.0081 ± 0.0019	0.093 ± 0.020	0.608 ± 0.173
$P_{PG}A/V_{wo}$	0.0084 ± 0.0020	0.157 ± 0.083	1.643 ± 0.518
$P_{EG}A/V_{wo}$	0.0045 ± 0.0020	0.069 ± 0.020	0.281 ± 0.029

Table 2.2. *Hydraulic conductivity, which describes the membrane permeability to water, when in conjuction with DMSO, propylene glycol (PG), and ethylene glycol (EG) at three different temperatures.*

Hydraulic conductivity (µm/Pa*s) x 10^8	**4°C**	**21°C**	**37°C**
$L_{P,DMSO}A/V_{wo}$	1.03 ± 0.11	3.74 ± 0.45	11.0 ± 1.7
$L_{P,PG}A/V_{wo}$	1.04 ± 0.17	4.82 ± 1.1	67.6 ± 42.8
$L_{P,EG}A/V_{wo}$	0.97 ± 0.11	3.97 ± 0.36	10.8 ± 0.88

The Arrhenius activation energy, described in *Equation 1.3*, can also be determined for each of the different CPAs. The activation energy (E_a) provides a measure of the energy barrier to water transport across the membrane. This value is determined by plotting $ln(L_P \text{ or } P_S)$ vs. $1/T$, as shown in *Figure 2.5*.

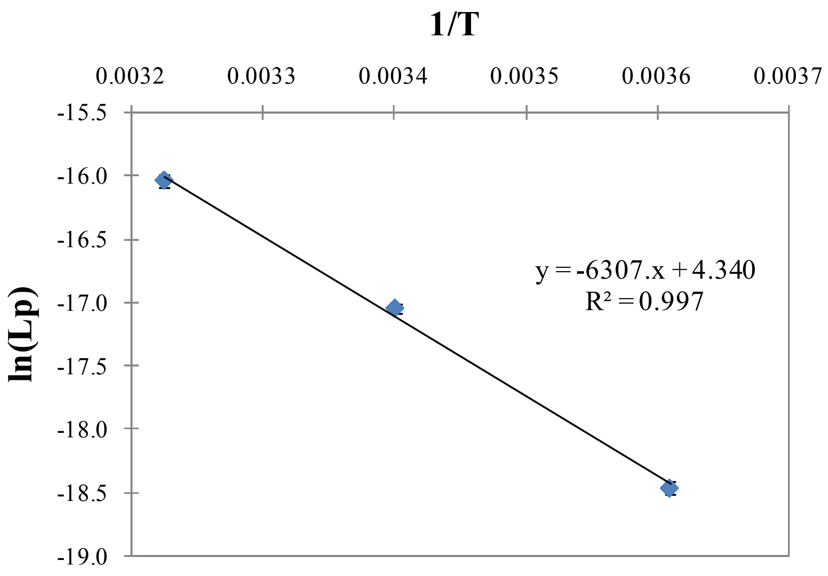

Figure 2.5. *An example of the plot used to determine the permeability activation energy. This graph gives the water permeability activation energy in the presence of ethylene glycol. The slope of the graph is multiplied by the ideal gas constant in order to determine the activation energy.*

The slope of this relationship is multiplied by the gas constant *R* in order to determine the activation energy. A summary of these values is shown in *Table 2.3*.

Table 2.3. *The Arrhenius activation energies for water and CPA permeability*

Cryoprotectant	**Water permeability activation energy (kJ/mol)**	**CPA permeability activation energy (kJ/mol)**
DMSO	51.9	95.6
Propylene glycol	66.8	108.9
Ethylene glycol	53.4	116.4

These permeability parameters can be utilized when designing optimal procedures for adding and removing cryoprotectant chemicals. The permeability characteristics of the membrane indicate how fast the water and CPA are able to cross the cell membrane. This in turn can be used to determine how long it will take for the cell volume to equilibrate when place in an anisotonic solution. In addition, these parameters are useful for predicting water transport during freezing, as described by *Equation 1.10*.

CHAPTER 3 – DETERMINATION OF OSMOTIC TOLERANCE LIMITS:

In order to design an optimized procedure for the addition and removal of cryoprotectant chemicals, it is necessary to determine the osmotic tolerance limits of the cells. This ensures that the cells will remain in a volume range that corresponds to maintained functional integrity. In these experiments, neurons were exposed to seven different solutions, with osmolarities ranging from 5 to 7000 mOsm. The viability of the cells was determined directly following exposure in addition to one day following exposure.

Experimental methods:

Cell culture

The cells used in the experiments are from Neuroscreen-1 (NS1) cell line, a subclone of the PC12 cell line which is a standard model system for neurons. NS1 cells were cultured in tissue culture flasks containing DMEM media with horse serum and Pen/Strep at 37°C in a 5% CO_2 environment. NGF-β, a nerve growth factor recombinantly produced in rats (Sigma N2513), was added at a concentration of 50 μg/mL in order to transform the neural progenitor cells into neurons. For the osmotic tolerance experiments, cells were seeded onto 25 mm diameter glass cover slips, coated with poly-L-lysine and collagen. They were cultured in 35 mm Petri dishes for 2 days before experimentation.

Solution preparation

The solutions were prepared to only contain non-permeating solutes. For the hypotonic solutions (< 300 mOsm), 1X PBS with Ca^{2+} and Mg^{2+} was diluted with purified DI water. For the hypertonic solutions (> 300 mOsm), 1X PBS was supplemented with NaCl. The osmolarity was confirmed using an Advanced Instruments freezing point depression micro-osmometer. The micro-osmometer can only measure osmolarities up to 1000 mOsm, so the higher concentration solutions were diluted with purified DI water in order to measure the concentration. The solutions were adjusted to a pH of 7.0.

Phase contrast imaging

A phase contrast inverted microscope and a Qicam camera are used to take "before" images of each cover slip using a 10x objective. Ten randomly selected areas on the cover slip are imaged and counted to determine the baseline cell density before the cells have been exposed to any solutions. For the overnight experiments, images are taken before the solution has been applied and on the second day before the cells are incubated in dye and imaged. An example of a typical phase contrast image is shown in *Figure 3.1*.

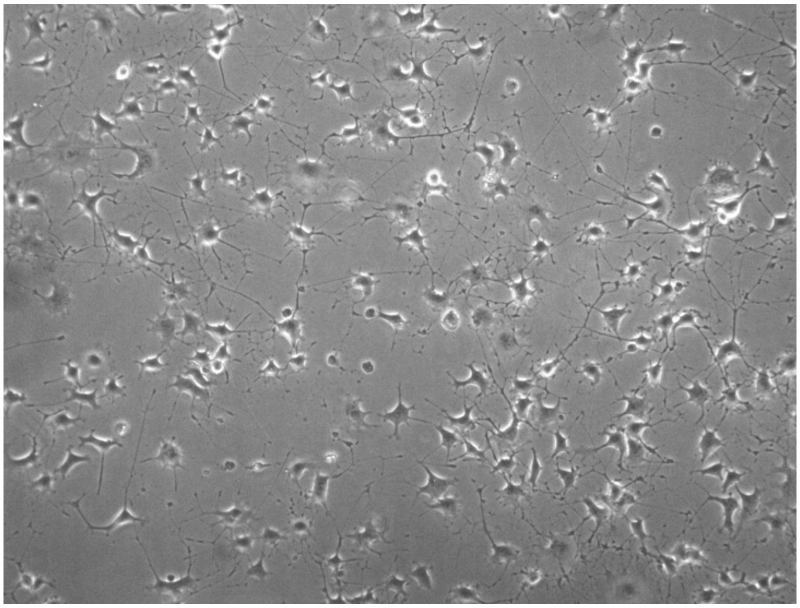

Figure 3.1. *A typical phase contrast image of the NS1 cells before any solution has been applied.*

Cell exposure to solutions

Cells were incubated in the appropriate solution for 15 minutes. The overnight samples were then provided with media and NGF and placed back in the incubator. The instant samples were incubated in 1.25 µg/mL calcein-AM and 2 µM ethidium homodimer for an additional 15 minutes before imaging. The next day, the overnight samples were incubated in the same calcein-AM/ethidium homodimer solution and imaged. Each experiment was performed in quadruplicate, giving eight samples total at each concentration (four instantaneously and four overnight).

Live/dead staining

In order to determine cell viability following exposure to the different solutions, a live/dead staining approach was utilized. Calcein-AM, the same dye used in the fluorescence quenching experiments, is used as the live stain, and ethidium homodimer is used as the dead stain. Calcein-AM is converted to calcein by esterases inside the cell, leaving the molecule unable to permeate out of the cell membrane. Only calcein is fluorescent, and since these esterases are only active in living cells, only living cells will fluoresce. The dye is excited by green light (490 nm) and emits green light (520 nm). The mechanism for live staining is shown in *Figure 3.2*.

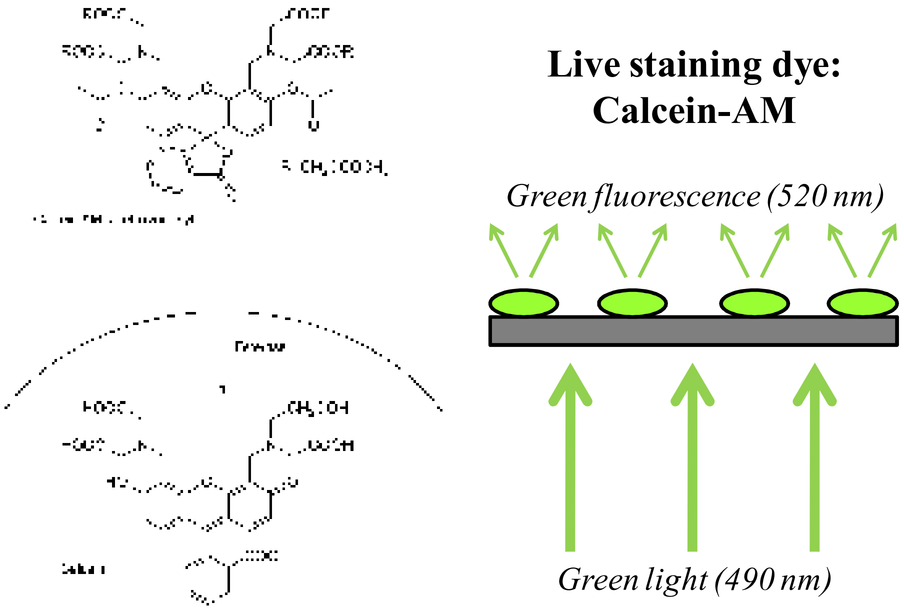

Figure 3.2. *The mechanism of action for the "live" stain. Calcein-AM is converted to calcein inside the cell, a fluorescent molecule which emits green light when excited by green light.*

Ethidium homodimer is used as the dead stain. It is impermeable to the cell and will therefore only be found in dead cells with leaky membranes. The dye intercalates with the DNA in the cell, fluorescing red light when excited with blue light. The mechanism is shown in *Figure 3.3*.

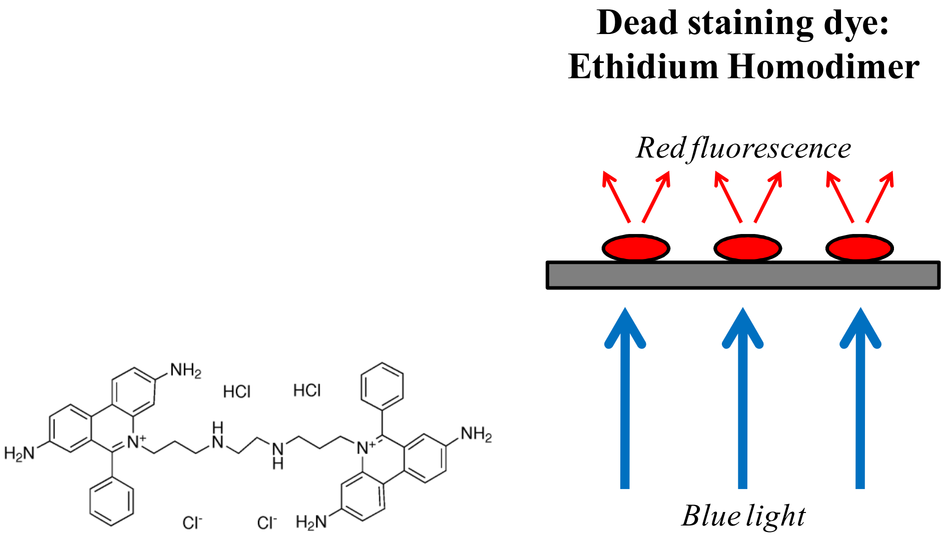
Dead staining dye:
Ethidium Homodimer
Red fluorescence
Blue light
NH2
HCl
HCl
H2N
N+
H
N
N
H
N+
NH2
Cl-
Cl-
H2N

Figure 3.3. *The mechanism of action for the "dead" stain. Ethidium homodimer is only able to permeate the membranes of dead cells, where it intercalates with the DNA. It emits red dye when excited with blue light.*

Once the cells have been incubated in the dye, they are imaged using a 10x objective along with a Qicam camera and Image Pro software. Five randomly selected areas on the cover slip are imaged under both green and blue light. The number of viable and dead cells is then counted for each area. Examples of typical live and dead stain images are shown in *Figure 3.4*.

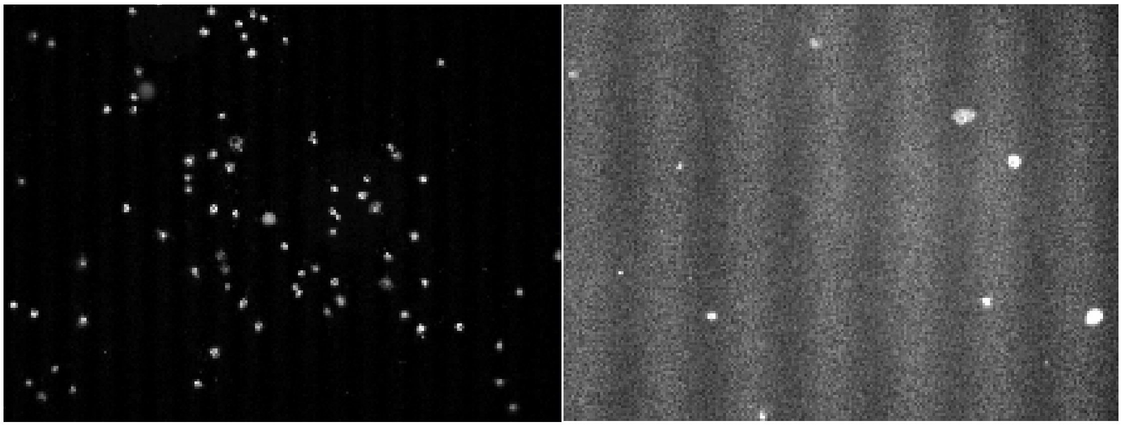

Figure 3.4. *A typical live stain image (left) and dead stain image (right) of the NS1 cells.*

Experimental results and discussion:

Data analysis was performed by counting the number of cells in the "before" images, the number of live cells, and the number of dead cells. All cell counting data is available in *Tables AI.1 – AI.6* in *Appendix I*. The first preliminary analysis of the osmotic tolerance data indicated high cell viability even when cells were exposed to strongly anisotonic solutions. This percentage of live cells, shown in *Figure 3.5*, was calculated by dividing the number of live cells by the total number of live and dead cells. The error bars represent the standard error of the mean of the quadruplicate measurement.

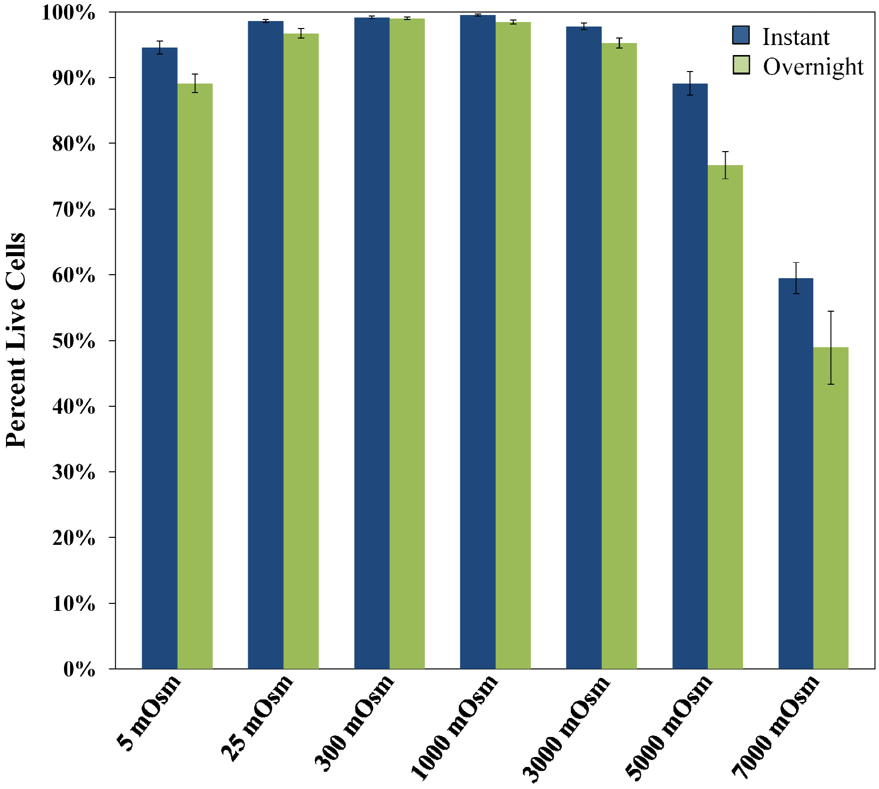

Figure 3.5. *The percentage of live cells when calculated by dividing the number of live cells by the total number of live and dead cells. The error bars represent the standard error of the mean of the quadruplicate measurement.*

However, this high value of cell viability is suspect, as cells should experience more severe damage when exposed to such hypotonic and hypertonic solutions. After closer examination, it appears that many cells were detaching from the cover slips after exposure to the solutions, giving artificially high cell viability values. For example, the difference between the cell density from Day 1 (before any solution had been applied to the cells) and Day 2 (after solution had been applied but before live/dead staining) for the overnight samples is shown in *Figure 3.6*. The percent difference was calculated by finding the difference in cell density from Day 1 to Day 2 and dividing by the Day 1 cell density. The error bars represent the standard error of the mean of the quadruplicate measurement. The cells that were exposed to solutions at or near isotonic conditions had a net positive change, indicating that cells continued to grow and divide. The cells that were exposed to solutions far from isotonic conditions exhibited a net negative change, indicating that cells were not growing and were detaching from the cover slip.

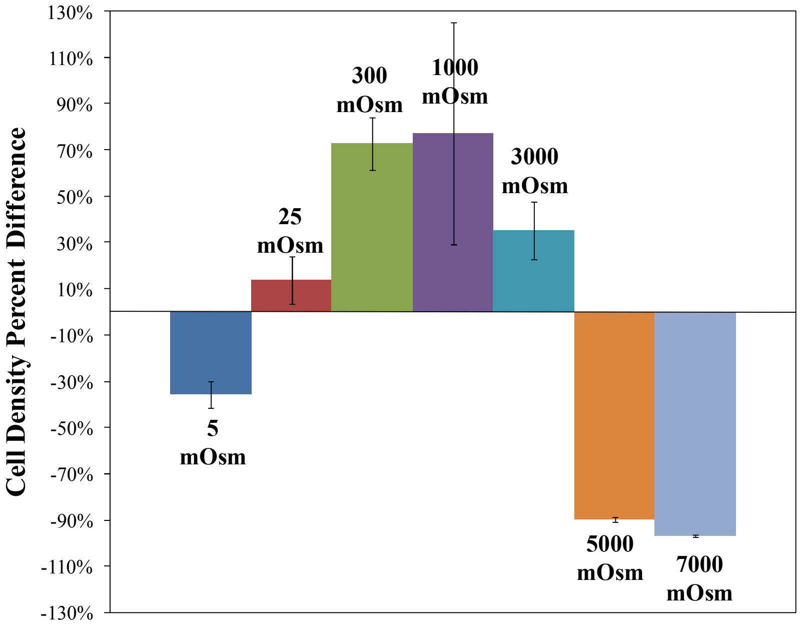

Figure 3.6. *Phase contrast images were taken of the overnight samples on Day 1 (before any solution was applied) and on Day 2 (after solution was applied but before live/dead staining). This figure shows the percent difference in cell density from Day 1 to Day 2. Those cells that were exposed to solutions at or near isotonic conditions showed growth, while those cells that were exposed to solutions far from isotonic conditions showed a loss of cells, indicating that cells were becoming detached.*

Though the precise mechanism is unclear, it is assumed that those cells that were lost became detached due to cellular damage or death. It is vital that cells remain attached to the surface when CPA solutions are added before cryopreservation, or they will be considered lost whether or not they are actually dead.

In order to account for this loss, the remaining viability of the cells was determined by defining a parameter for cell yield. This is calculated by dividing the number of live cells by the average cell density before solution was added. The control (300 mOsm isotonic solution) gave approximately 20% growth between the initial phase contrast image and the live/dead imaging (total number of live and dead cells). In order to account for this, both the instant and overnight data were normalized to the control. The results are shown in *Figure 3.7*, with the error bars indicating the standard error of the mean of the quadruplicate measurement.

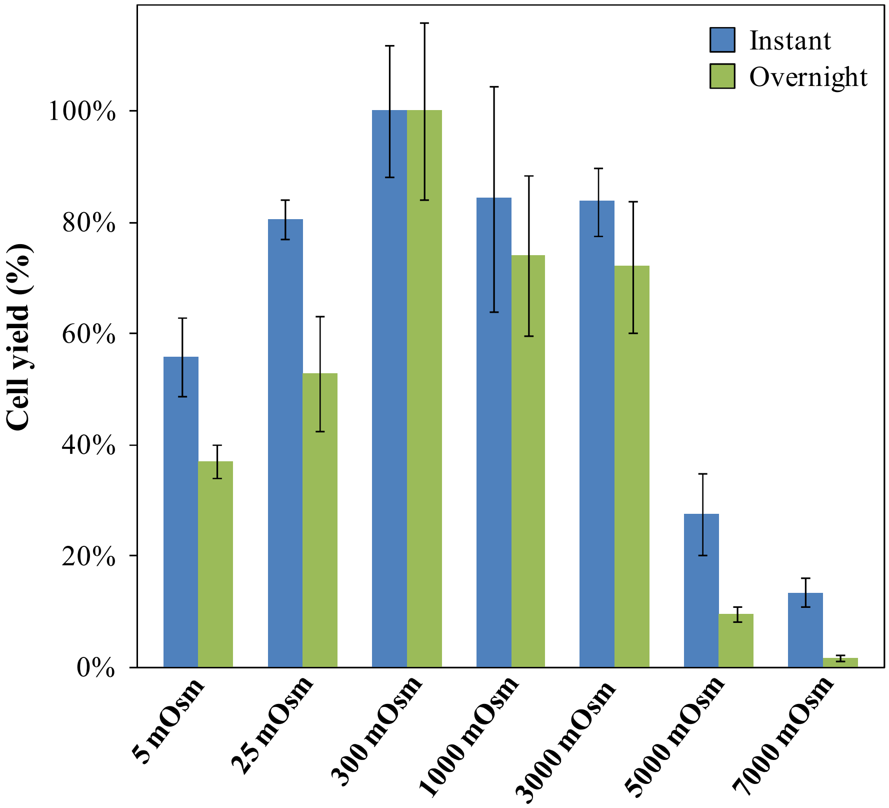

Figure 3.7. *In order to account for detached cells, the data was for each solution was normalized to the control (300 mOsm isotonic solution). The error bars represent the standard error of the mean of the quadruplicate measurement.*

The cell viability appears dramatically lower when the detached cells are accounted for, much closer to the expected result.

In general, it appears that the cell viability decreases with the overnight samples, indicating that it may take time for the damage to be incurred. However, t-test statistics only show a statistically significant difference in the means (to 95% confidence) for the 5 mOsm samples and 7000 mOsm samples. This indicates that the effects may be more severe as the solution becomes farther from isotonic. For a summary of these two-sample comparisons, see *Table AII.1* in *Appendix II.*

A one-way ANOVA analysis was also performed to see if there is a statistically significant difference in the cell yield given by the different solutions. For both the instant and overnight samples, the overall difference was found to be statistically significant to 95% confidence (see *Tables AII.2* and *AII.4* in *Appendix II*). Multiple range testing (LSD) was also performed to assess the difference in cell yield between individual solutions. The results of these analyses are shown in *Tables AII.3* and *AII.5* in *Appendix II*. The overnight samples gave 13 pairs that were significantly different to 95% confidence, while the instant samples gave 10 pairs that were significantly different to 95% confidence. This may indicate that the differences in viability are more dramatic with longer exposure.

This data indicates that approximately 50% of the cells will remain viable and attached to the surface when exposed to solutions ranging from 25 – 3000 mOsm. Using the Boyle-van't Hoff relationship described in *Equation 1.5*, the relative change in the osmotically active volume can be determined for each extracellular concentration of solute. The trend predicted from this relationship is shown in *Figure 3.8*.

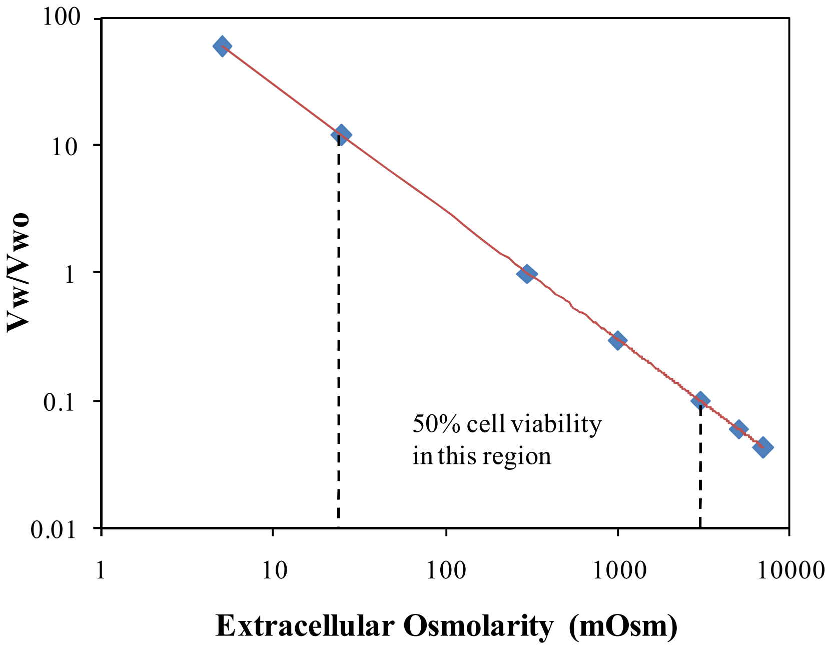

Figure 3.8. *The relative change in the osmotically active cell volume with exposure to different extracellular osmolarities, as predicted by the Boyle-van't Hoff relationship.*

From this relationship and the assumption that 50% of cells remain viable and attached between the extracellular concentrations of 25 and 3000 mOsm, the equilibrium cell volume change can be calculated to be 0.1x to 12x the original cell volume. However, the 15 minutes of exposure is probably not sufficient time for the cells to reach these extreme volume changes. The permeability parameters determined in *Chapter 2* can be used to predict how much the volume actually changed in this short period of exposure.

These ranges give a starting point for determining optimal procedures for addition and removal of CPA without causing cell damage due to osmotic pressure differences. However, more concentrations closer to isotonic conditions need to be assessed in order to narrow this range to one that gives a higher cell yield.

CHAPTER 4 – DEVELOPMENT OF A NOVEL CPA ADDITION AND REMOVAL METHOD:

Traditionally, cryoprotectant chemicals have been added in increasing concentration steps to avoid excessive shrinking of the cells. In this procedure, time is allowed after each step for the cell to reach equilibrium. As a result, the procedure can take a long period of time, up to several hours. A more efficient way to do this, as shown in *Figure 4.1* below, is to exponentially increase or decrease the concentration of cryoprotectant with time (shown in black). Since an exponential change can be difficult to control, a linear approximation of the curve can be performed instead (shown in grey). These procedures would take on the order of minutes rather than hours.

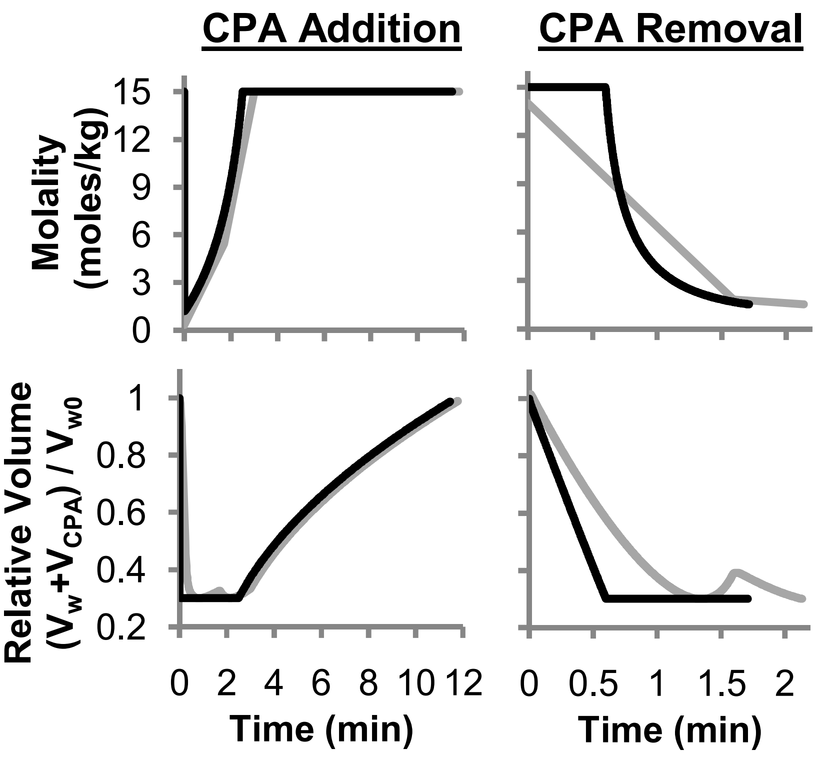

Figure 4.1. *A novel method for adding and removing CPAs to and from cells would utilize a constantly changing CPA concentration rather than a stepwise change.*

In order to examine the feasibility of this delivery method, a system needs to be developed which utilizes the current experimental apparatus. The primary pieces of equipment in the system are the syringe pumps used to deliver solutions to cells. To test whether the syringe pumps are capable of accurately pumping a varying concentration, experiments were performed with red dye and the flow chamber used in the fluorescence quenching experiments. One syringe pump was filled with water while the other was filled with dye. The pumps were programmed to linearly change their rates, keeping the total flow rate constant, so that the concentration would be changed in a linear fashion. The solution was passed through the channel in the flow chamber (see *Figures 2.1* and *2.2*) so that the microscope could track the change in intensity with time.

Intensity vs. dye concentration calibration curve

The relationship between dye concentration and intensity may not be linear for all concentrations. Therefore, a calibration curve was created to find the linear range. In these experiments, a dye solution of a known concentration was perfused through the flow chamber for one minute. The average intensity over the course of approximately 60 data points was recorded at four different imaging settings: 1x1 binning (976 µs exposure), 2x2 binning (244 µs exposure), 4x4 binning (61µs exposure), and 8x8 binning (15 µs exposure). The differing exposure times of the camera changes the resulting light intensity values. The results of the calibration curve are shown in *Figure 4.2*. There appears to be little correlation between dye concentration and intensity at low concentrations. However, the relationship appears to be linear in the range of 2-16% dye. Therefore, these are the concentrations that should be used during experimentation. The slope of the relationship is negative because as more dye flows, less light is able to reach the objective, which decreases the intensity.

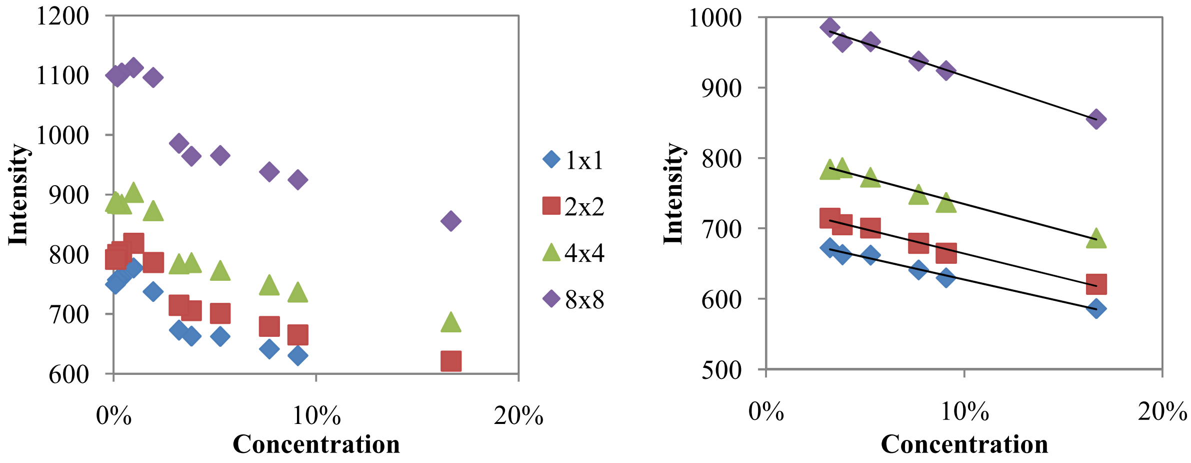

Figure 4.2. *A calibration curve was created to determine the linear region of intensity vs. dye concentration. Low concentrations did not give significantly different intensity values, as seen in the left figure. The linear region is shown on the right figure and appears to be in the range of 2-16% dye.*

Experimental results and discussion:

Once the linear range was established, experimentation with the syringe pumps could begin. The syringe pumps were programmed to pump at changing rates that would give two linear regions of increasing intensity with different slopes. There were several problems commonly encountered which caused the data to deviate from the expected results. Each of these is shown visually in *Figure 4.3*. The first common problem was a lag time at the beginning of pumping. If the syringe was programmed to start pumping from a flow rate of zero, it appeared to lack the momentum to actually begin pumping. A set of data in which this problem was encountered is shown in *Figure 4.3.(a)*.This problem can be improved by beginning pumping at a non-zero flow rate. The second common problem was that the plunger of the syringe would sometimes get stuck, then suddenly jerk forward. A set of data in which this problem was encountered is shown in *Figure 4.3.(b)*.This problem can be alleviated by using a new syringe each time so the lubrication is not worn down.

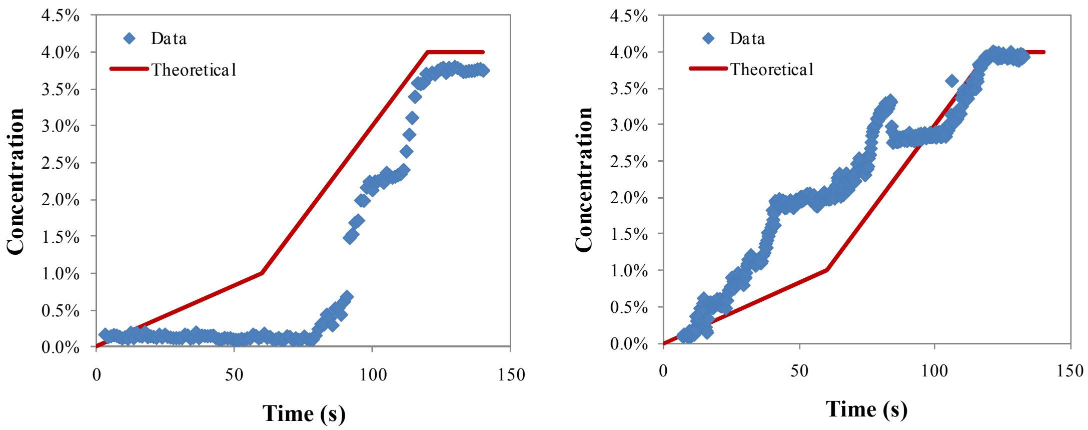

Figure 4.3. *Visual representations of two commonly encountered problems. In the figure on the left (a), a lag time is experienced at the beginning of pumping. In the figure on the right (b), the syringe gets stuck and jerky due to a wearing down of the lubrication.*

One concern is that the solution may not be evenly mixed throughout the channel, causing cells to be exposed to a concentration gradient. To predict whether there is enough time for the solution to be well-mixed, *Equations 4.1*, *4.2*, and *4.3* can be applied. The variables t_d and t_r refer to the diffusion time and the residence time, respectively. Assuming the mixing is diffusion limited, the ratio of t_d/t_r should be less than or equal to one for the solution to be well-mixed. R refers to the tube radius, D refers to the diffusion coefficient of the dye in water, l refers to the length of the tube, and F refers to the flow rate.

$$t_d = \frac{R^2}{D} \qquad [4.1]$$

$$t_r = \frac{\pi R^2 l}{F} \qquad [4.2]$$

$$\frac{t_d}{t_r} = \frac{F}{D\pi l} \leq 1 \qquad [4.3]$$

In order to maximize the t_d/t_r ratio, a low flow rate and long tubing length for mixing should be utilized. However, using too low of a flow rate will negatively impact the ability of the syringe pumps to instantaneously change the solution concentration. In order to improve mixing, a micromixer was used. This appeared to decrease the noise of the data, though problems were encountered in which the micromixer became clogged with air bubbles, making it hard to regulate the flow.

Once the lag time, low lubrication, and mixing issues were addressed, the syringes were able to deliver solutions as desired. The results of an experiment using the flow chamber, microscope, and camera are shown in *Figure 4.4*. There is some noise, however the concentration is clearly following the theoretical path.

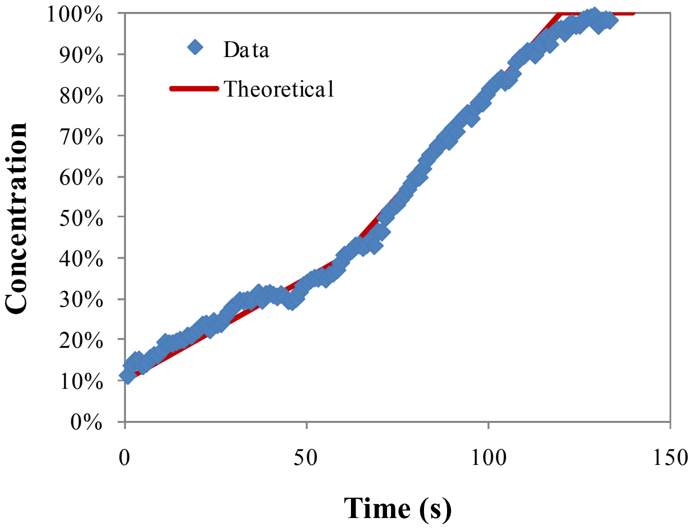

Figure 4.4. *The intensity data (converted to concentration through the linear relationship) versus time using the syringe pumps to vary the concentration of dye in a controlled manner.*

In order to confirm that the concentrations were varying as desired, experiments were also performed with a salt solution. The flow chamber was dismantled so that the channel outlet was collected in a microcentrifuge tube. Twenty seconds of flow was collected in each tube for a total of 240 seconds and 12 samples. A freezing point depression micro-osmometer was then used to measure the concentration in each tube. The results of this experiment are shown in *Figure 4.5*. The concentrations follow the theoretical concentration line very well, improving confidence that the experimental system can successfully deliver varying concentrations.

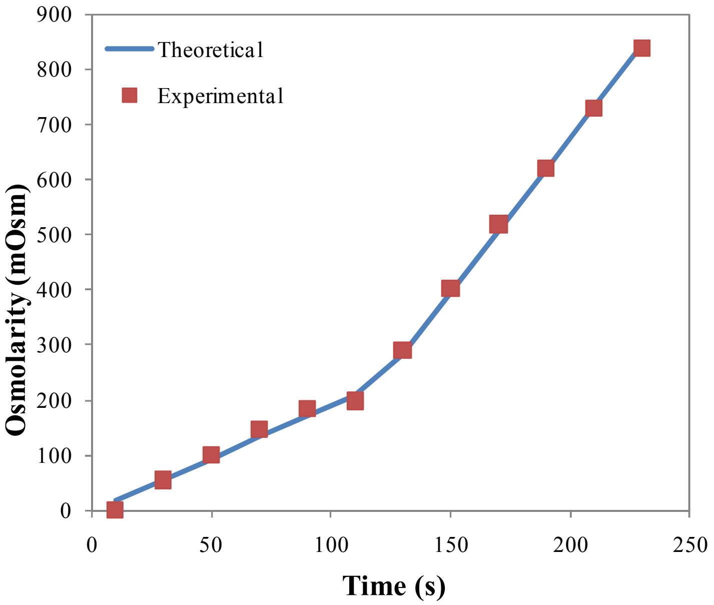

Figure 4.5. *The salt concentration data versus time using the syringe pumps to vary the concentration of salt solution in a controlled manner.*

Now that the capability of the system to controllably deliver changing solution concentrations has been shown, further experimentation is needed to see how this method of CPA addition affects cell viability. This could be performed by using the flow chamber to deliver CPA in the desired way. The gasket can be modified so that instead of a narrow channel, a circular opening is available so that almost the entire cover slip of cells is exposed to the solution. This can be followed by live/dead staining of the cover slip to assess cell viability. Further characterization of mixing in the circular channel may be necessary to ensure that no concentration gradients are forming. Overall, this novel method of adding cryoprotectant chemicals to cells could greatly improve the efficiency of CPA addition prior to cryopreservation.

CHAPTER 5 – CONCLUSIONS AND FUTURE DIRECTIONS:

This thesis focused on characterizing the membrane permeability and osmotic tolerance limits for adherent neurons so that optimal methods for delivering cryoprotectant chemicals can be created. In addition, preliminary work was performed on examining the feasibility of a novel procedure for addition of CPAs which would greatly improve process efficiency. Throughout the project, the concepts of membrane permeability and transport have been essential in understanding the system.

The preliminary data for the membrane permeability and osmotic tolerance limits of the NS1 cells can be used to design initial procedures for optimal delivery of cryoprotectant chemicals. This can be done using mathematical modeling which assesses the change in volume of the cells when exposed to various solutions. The osmotic tolerance limits define the volume range which maintains high cell viability, while the permeability parameters are essential for modeling membrane transport.

The osmotic tolerance limits determined through experimentation define a very broad range of cell viability. Because initial data showed high cell survival even at strongly anisotonic conditions, more solutions closer to isotonic conditions were not examined. However, closer examination of the data showed that cell viability was lower than initially presumed due to the detaching of cells from the surface. In order to design truly optimal procedures for adding and removing CPAs, it will be necessary to define clearer osmotic tolerance limits where cell viability remains greater than 90% after exposure. This will be performed by testing more concentrations closer to isotonic conditions in order to narrow this range and give a higher cell yield.

In addition, the linear concentration change method of adding CPAs to cells needs to be tested to examine if cell viability follows the predicted trend. If this method can be used to add and remove cryoprotectant chemicals, the efficiency of the process would be greatly improved.

REFERENCES:

Alberts, B. et al. (2008). *Molecular biology of the cell*. New York: Garland Science.

Arakawa, T. et al. (1990). The basis for toxicity of certain cryoprotectants: a hypothesis. *Cryobiology*, *27*(4), 401-415.

Bischof, J.C. (2000). Quantitative measurement and prediction of biophysical response during freezing in tissues. *Annual Review of Biomedical Engineering*, *2*, 257-288.

Devireddy, R.V. et al. (2000). The effect of extracellular ice and cryoprotective agents on the water permeability parameters of human sperm plasma membrane during freezing. *Human Reproduction*, *15*(5), 1125-1135.

Diller, K.R. (1975). Intracellular freezing: effect of extracellular supercooling. *Cryobiology*, *12*(5), 480-485.

Hamaan, S. et al. (2002). Measurement of cell volume changes by fluorescence self-quenching. *Journal of Fluorescence*, *12*(2), 139-145.

Karlsson, J.O.M. et al. (1993). Nucleation and growth of ice crystals inside cultured hepatocytes during freezing in the presence of dimethyl sulfoxide. *Biophysical Journal*, *65*, 2524-2536.

Karlsson, J.O.M., Cravalho, E.G., & Toner, M. (1994). A model of diffusion-limited ice growth inside biological cells during freezing. *Journal of Applied Physics*, *75*(9), 4442-4455.

Karlsson, J.O.M. & Toner, M. (1996). Long-term storage of tissues by cryopreservation: critical issues. *Biomaterials*, *17*(3), 243-256.

Levin, R.L., Cravalho, E.G., & Huggins, C.E. (1976). A membrane model describing the effect of temperature on the water conductivity of erythrocyte membranes at subzero temperatures. *Cryobiology*, *13*(4), 415-429.

Mazur, P. (1963). Kinetics of water loss from cells at subzero temperatures and the likelihood of intracellular freezing. *Journal of General Physiology*, *47*, 347-369.

Mazur, P. (1970). Cryobiology: the freezing of biological systems. *Science*, *168*(3934), 939-949.

Mazur, P. (1977). The role of intracellular freezing in the death of cells cooled at supraoptimal rates. *Cryobiology*, *14*(3), 251-272.

Mazur, P. (1984). Freezing of living cells: mechanisms and implications. *American Journal of Physiology - Cell Physiology*, *247*(3), C125-C142.

McGrath, J.J. (1997). Quantitative measurement of cell membrane transport: technology and applications. *Cryobiology*, *34*, 315-334.

Meryman, H.T. (1974). Freezing injury and its prevention in living cells. *Annual Review of Biophysics and Bioengineering*, *3*, 341-363.

Solenov, E. et al. (2004). Sevenfold-reduced osmotic water permeability in primary astrocyte cultures from AQP-4 deficient mice, measured by a fluorescence quenching method. *American Journal of Physiology - Cell Physiology*, *286*, C426-C432.

Stein, W.D. (1967). *The movement of molecules across cell membranes*. New York: Academic Press.

Tortora, G.J. & Derrickson, B. (2009). *Principles of anatomy and physiology*. Hoboken, NJ: John Wiley & Sons.

Verkman, A.S. (2000). Water permeability measurement in living cells and complex tissues. *Journal of Membrane Biology*, *173*, 73-87.

APPENDICES

APPENDIX I. OSMOTIC TOLERANCE RAW DATA

Table AI.1. *Raw data from osmotic tolerance tests for overnight samples (1 of 4)*

		Ethanol		Isotonic									
		1		2		3		4		5		6	
		Day 1	Day 2	Day 1	Day 2	Day 1	Day 2	Day 1	Day 2	Day 1	Day 2	Day 1	Day 2
Phase Contrast	1	152	269	192	272	114	335	102	158	171	163	160	160
	2	90	184	189	161	120	283	53	158	76	161	68	91
	3	100	209	128	112	79	197	64	66	120	137	64	96
	4	172	238	228	111	103	179	74	173	52	122	99	73
	5	80	144	195	78	142	87	71	63	48	116	77	116
	6	174	195	310	340	120	176	131	169	80	98	133	214
	7	188	167	226	215	134	208	94	154	86	86	66	222
	8	127	201	173	372	99	219	71	131	64	124	93	128
	9	199	157	97	342	143	177	44	178	89	118	58	146
	10	119	291	161	313	100	250	64	157	74	152	67	139
Live	1		0		223		247		152		168		176
	2		0		237		290		142		279		74
	3		0		53		203		112		82		89
	4		0		104		195		45		88		134
	5		0		189		205		165		91		150
Dead	1		260		3		3		2		5		2
	2		185		3		2		2		3		2
	3		154		0		1		0		0		0
	4		71		2		4		0		0		1
	5		27		5		3		0		0		0

Table AI.2. *Raw data from osmotic tolerance tests for overnight samples (2 of 4)*

		5 mOsm								25 mOsm							
		7		8		9		10		11		12		13		14	
		Day 1	Day 2	Day 1	Day 2	Day 1	Day 2	Day 1	Day 2	Day 1	Day 2	Day 1	Day 2	Day 1	Day 2	Day 1	Day 2
Phase Contrast	1	84	65	89	21	190	133	36	25	174	128	215	202	313	203	103	401
	2	100	56	103	33	149	101	68	43	93	91	192	324	277	69	169	322
	3	86	57	95	25	152	74	72	39	79	101	146	175	127	18	194	227
	4	87	48	67	27	121	95	44	32	135	203	112	162	259	323	207	270
	5	109	51	90	48	88	75	106	14	110	204	108	245	198	197	190	170
	6	103	54	85	56	128	212	67	31	148	140	97	138	204	151	161	297
	7	124	65	62	113	216	100	76	43	186	126	95	66	189	136	198	280
	8	153	103	129	42	208	163	30	37	177	122	129	107	267	135	196	336
	9	125	63	113	29	196	95	39	35	113	103	276	53	192	239	345	220
	10	187	70	111	47		112	65	93	117	100	147	107	171	198	264	315
Live	1		77		63		133		22		142		256		132		281
	2		55		28		162		28		108		133		13		252
	3		56		44		73		37		76		44		6		249
	4		40		69		80		51		81		93		101		135
	5		37		47		89		31		87		99		214		276
Dead	1		5		6		9		0		4		9		3		5
	2		5		1		15		9		9		5		0		5
	3		5		9		4		10		3		1		1		6
	4		3		13		5		8		4		3		2		1
	5		7		8		11		6		1		5		4		2

Table AI.3. *Raw data from osmotic tolerance tests for overnight samples (3 of 4)*

		990 mOsm								3028 mOsm							
		15		16		17		18		19		20		21		22	
		Day 1	Day 2	Day 1	Day 2	Day 1	Day 2	Day 1	Day 2	Day 1	Day 2	Day 1	Day 2	Day 1	Day 2	Day 1	Day 2
Phase Contrast	1	158	205	196	93	289	134	69	102	269	148	66	206	86	43	95	143
	2	182	113	162	135	165	101	43	137	154	124	88	129	123	47	101	166
	3	85	105	79	214	183	81	59	109	98	116	98	163	76	109	86	156
	4	111	138	131	116	258	187	67	198	92	131	78	241	78	118	91	75
	5	130	187	161	164	103	95	99	110	80	88	68	113	36	156	96	155
	6	110	140	149	184	248	181	92	149	107	103	111	256	162	187	130	104
	7	91	108	241	183	142	213	71	61	90	88	97	166	119	169	102	90
	8	198	148	167	232	185	159	41	152	145	180	104	215	201	167	106	87
	9	159	112	185	127	115	72	8	156	169	90	237	148	161	112	131	110
	10	191	87	142	170	161	136	43	236	133	132	136	241	243	170	77	84
Live	1		137		227		218		84		102		246		101		95
	2		75		150		317		84		103		132		206		95
	3		30		215		153		98		65		98		140		100
	4		140		96		45		110		51		134		167		102
	5		129		82		219		133		106		205		116		131
Dead	1		1		0		5		0		5		14		18		2
	2		3		1		2		1		3		6		9		2
	3		0		2		1		2		1		2		13		2
	4		3		4		1		2		2		2		15		3
	5		4		2		0		3		7		12		11		4

Table AI.4. *Raw data from osmotic tolerance tests for overnight samples (4 of 4)*

		4767 mOsm								7085 mOsm					
		23		24		25		26		27		28		29	
		Day 1	Day 2	Day 1	Day 2	Day 1	Day 2	Day 1	Day 2	Day 1	Day 2	Day 1	Day 2	Day 1	Day 2
Phase Contrast	1	195	15	191	18	128	11	57	7	60	7	98	1	180	6
	2	113	12	159	20	78	11	32	6	145	4	89	2	243	4
	3	54	14	206	9	80	19	45	7	113	4	87	2	138	2
	4	106	16	102	15	114	3	56	10	91	3	66	1	88	0
	5	100	17	88	1	57	5	80	4	62	5	87	1	74	3
	6	106	25	131	10	139	6	57	7	232	9	86	3	82	1
	7	96	11	109	8	107	2	45	10	175	2	109	1	87	5
	8	77	7	263	7	229	7	59	2	273	8	193	0	239	3
	9	69	2	317	20	288	16	102	10	176	5	137	5	155	2
	10	130	12	239	22	209	15	145	6	202	6	140	11	101	3
Live	1		33		18		20		13		4		1		1
	2		17		25		17		10		3		0		3
	3		15		15		10		9		7		3		2
	4		13		25		15		15		7		5		2
	5		9		21		12		16		8		1		4
Dead	1		5		5		8		0		3		1		0
	2		2		9		6		4		3		2		2
	3		2		10		6		2		8		5		2
	4		3		11		6		5		4		5		4
	5		3		8		4		5		7		3		3

Table AI.5. *Raw data from osmotic tolerance tests for instant samples (1 of 2)*

		Ethanol	Isotonic				5 mOsm				25 mOsm			
		1	2	3	4	5	6	7	8	9	10	11	12	13
Phase Contrast	1	61	44	43	54	99	102	45	54	27		69	84	94
	2	30	52	56	61	95	57	38	82	78		85	50	75
	3	40	53	80	66	107	65	22	36	58		72	90	65
	4	50	40	44	92	103	152	71	89	41		103	54	65
	5	45	58	35	43	161	105	57	72	92		74	67	40
	6	67	94	75	82	97	150	55	80	35		137	92	91
	7	86	82	54	70	136	140	77	68	43		160	81	107
	8	31	35	64	73	94	52	29	153	30		116	60	76
	9	44	55	89	62	81	77	27	76	9		25	97	151
	10	41	33	71	59	74	83	23	59	21		65	74	82
Live	1	0	103	47	53	154	90	40	49	20	108	83	90	72
	2	0	80	80	56	93	98	31	76	27	78	90	66	41
	3	0	107	71	61	121	131	7	39	18	73	63	64	67
	4	0	69	39	74	122	46	19	58	16	84	84	67	184
	5	0	80	72	83	148	76	30	50	31	68	85	79	78
Dead	1	63	2	1	1	0	8	0	0	1	2	0	1	1
	2	51	2	1	0	1	5	1	2	3	1	2	1	0
	3	23	0	0	0	0	4	1	0	2	1	0	1	2
	4	42	1	0	0	0	5	0	3	3	0	3	2	0
	5	117	0	1	2	1	2	1	2	3	1	2	1	1

Table AI.6. *Raw data from osmotic tolerance tests for instant samples (2 of 2)*

		990 mOsm				3028 mOsm				4767 mOsm				7085 mOsm			
		14	15	16	17	18	19	20	21	22	23	24	26	27	28	29	30
Phase Contrast	1	100	56	41	59	28	148	106	105	94	112	110	51	37	81	38	163
	2	103	63	61	123	35	122	101	145	57	200	145	52	41	96	53	125
	3	102	82	75	76	54	96	68	60	63	191	100	28	40	46	25	42
	4	122	72	91	85	58	155	55	79	85	156	106	21	26	51	42	65
	5	92	83	54	64	39	203	70	84	76	191	99	92	17	48	37	103
	6	145	100	31	145	33	136	68	144	86	301	131	67	50	95	46	123
	7	136	51	148	67	60	115	87	82	241	174	166	65	27	188	34	137
	8	106	104	56	23	27	82	88	86	78	178	105	16	39	115	44	83
	9	152	60	36	79	65	108	179	81	102	287	79	16	23	107	42	108
	10	200	164	70	61	31	51	115	53	46	151	120	21	22	70	44	76
Live	1	124	194	35	16	50	77	111	80	7	81	20	4	3	12	4	12
	2	177	102	83	34	50	127	63	69	17	70	42	6	3	8	5	16
	3	125	107	31	33	51	210	83	78	41	123	72	5	3	16	7	14
	4	142	79	75	38		123	132	56	15	73	115	6	3	24	6	46
	5	108	204	66	64		106	77	93	16	66	60	13	3	17	6	37
Dead	1	1	1	0	0	2	1	1	0	2	9	4	1	3	5	2	11
	2	0	0	2	0	3	0	2	3	1	6	6	0	3	10	5	11
	3	0	0	0	0	1	1	1	2	4	9	9	0	1	4	5	11
	4	1	1	0	0		2	4	5	1	6	24	0	3	19	5	41
	5	1	2	0	1	0	0	1	0	1	10	13	5	1	8	3	31

APPENDIX II. STATISTICAL ANALYSIS

Table AII.1. *T-test comparison of instant and overnight osmotic tolerance data*

Solution	***p-value***	***Significant to 95% confidence?***
5 mOsm	0.0484	**Yes**
25 mOsm	0.0791	No
300 mOsm	0.9413	No
1000 mOsm	0.6924	No
3000 mOsm	0.4140	No
5000 mOsm	0.0542	No
7000 mOsm	0.0132	**Yes**

Table AII.2. *ANOVA comparison of instant osmotic tolerance solutions*

Source	***Sum of Squares***	***Df***	***Mean Square***	***F-Ratio***	***P-Value***
Between groups	2.50175	6	0.416958	9.90	0.0000
Within groups	0.842496	20	0.0421248		
Total (Corr.)	3.34424	26			

Table AII.3. *Multiple range testing (LSD) of instant osmotic tolerance solutions. An asterisk has been placed next to 10 pairs, indicating that these pairs show statistically significant differences at the 95.0% confidence level.*

Contrast	***Sig.***	***Difference***	***+/- Limits***
5 - Day 1 - 25 - Day 1		-0.247917	0.32699
5 - Day 1 - 300 - Day 1	*	-0.44175	0.302734
5 - Day 1 - 1000 - Day 1		-0.28425	0.302734
5 - Day 1 - 3000 - Day 1		-0.27925	0.302734
5 - Day 1 - 5000 - Day 1		0.28375	0.302734
5 - Day 1 - 7000 - Day 1	*	0.42375	0.302734
25 - Day 1 - 300 - Day 1		-0.193833	0.32699
25 - Day 1 - 1000 - Day 1		-0.0363333	0.32699
25 - Day 1 - 3000 - Day 1		-0.0313333	0.32699
25 - Day 1 - 5000 - Day 1	*	0.531667	0.32699
25 - Day 1 - 7000 - Day 1	*	0.671667	0.32699
300 - Day 1 - 1000 - Day 1		0.1575	0.302734
300 - Day 1 - 3000 - Day 1		0.1625	0.302734
300 - Day 1 - 5000 - Day 1	*	0.7255	0.302734
300 - Day 1 - 7000 - Day 1	*	0.8655	0.302734
1000 - Day 1 - 3000 - Day 1		0.005	0.302734
1000 - Day 1 - 5000 - Day 1	*	0.568	0.302734
1000 - Day 1 - 7000 - Day 1	*	0.708	0.302734
3000 - Day 1 - 5000 - Day 1	*	0.563	0.302734
3000 - Day 1 - 7000 - Day 1	*	0.703	0.302734
5000 - Day 1 - 7000 - Day 1		0.14	0.302734

Table AII.4. *ANOVA comparison of overnight osmotic tolerance solutions*

Source	*Sum of Squares*	*Df*	*Mean Square*	*F-Ratio*	*P-Value*
Between groups	2.90314	6	0.483857	11.24	0.0000
Within groups	0.861255	20	0.0430628		
Total (Corr.)	3.76439	26			

Table AII.5. *Multiple range testing (LSD) of overnight osmotic tolerance solutions. An asterisk has been placed next to 13 pairs, indicating that these pairs show statistically significant differences at the 95.0% confidence level.*

Contrast	*Sig.*	*Difference*	*+/- Limits*
5 - Day 2 - 25 - Day 2		-0.15825	0.306086
5 - Day 2 - 300 - Day 2	*	-0.6445	0.306086
5 - Day 2 - 1000 - Day 2	*	-0.369	0.306086
5 - Day 2 - 3000 - Day 2	*	-0.3495	0.306086
5 - Day 2 - 5000 - Day 2		0.275	0.306086
5 - Day 2 - 7000 - Day 2	*	0.353917	0.330611
25 - Day 2 - 300 - Day 2	*	-0.48625	0.306086
25 - Day 2 - 1000 - Day 2		-0.21075	0.306086
25 - Day 2 - 3000 - Day 2		-0.19125	0.306086
25 - Day 2 - 5000 - Day 2	*	0.43325	0.306086
25 - Day 2 - 7000 - Day 2	*	0.512167	0.330611
300 - Day 2 - 1000 - Day 2		0.2755	0.306086
300 - Day 2 - 3000 - Day 2		0.295	0.306086
300 - Day 2 - 5000 - Day 2	*	0.9195	0.306086
300 - Day 2 - 7000 - Day 2	*	0.998417	0.330611
1000 - Day 2 - 3000 - Day 2		0.0195	0.306086
1000 - Day 2 - 5000 - Day 2	*	0.644	0.306086
1000 - Day 2 - 7000 - Day 2	*	0.722917	0.330611
3000 - Day 2 - 5000 - Day 2	*	0.6245	0.306086
3000 - Day 2 - 7000 - Day 2	*	0.703417	0.330611
5000 - Day 2 - 7000 - Day 2		0.0789167	0.330611

.